Mitochondrial Transport in Axons with Multiple Branching Junctions: A Computational Study

Ivan A. Kuznetsov[(a), (b)] and Andrey V. Kuznetsov[(c)]

[(a)] Perelman School of Medicine, University of Pennsylvania, Philadelphia, PA 19104, USA

[(b)] Department of Bioengineering, University of Pennsylvania, Philadelphia, PA 19104, USA

[(c)] Department of Mechanical and Aerospace Engineering, North Carolina State University, Raleigh, NC 27695-7910, USA; e-mail: avkuznet@ncsu.edu

Abstract

We explore the impact of multiple branching junctions in axons on the mean age of mitochondria and their age density distributions in demand sites. The study looked at mitochondrial concentration, mean age, and age density distribution in relation to the distance from the soma. We developed models for a symmetric axon containing 14 demand sites and an asymmetric axon containing 10 demand sites. We examined how the concentration of mitochondria changes when an axon is divided into two branches at the branching junction. We also studied whether mitochondria concentrations in the branches are affected by what portion of mitochondrial flux goes into the upper branch and what portion goes into the lower branch. Additionally, we explored whether the distributions of mitochondria mean age and age density in branching axons are affected by how the mitochondria flux splits at the branching junction. Our findings elucidate the effects of axonal branching on mitochondria age. Mitochondria aging is the focus of this study as recent research suggests it may be involved in neurodegenerative disorders.

Keywords: neurodegeneration; mitochondrial aging; Parkinson's disease; large axonal arbors; computational biology

1. Introduction

Dopaminergic (DA) neurons in the substantia nigra pars compacta die during Parkinson's disease (PD) (Chinta and Andersen 2005; Guo et al. 2018; Xu et al. 2017). The axonal arbors of these neurons are large and unmyelinated, and the morphology of their axons is very complex with multiple branching junctions. In humans, a single DA axon can form more than a million synapses (Matsuda et al. 2009). Maintaining such a large arbor requires a lot of energy, and energy supply problems may be a possible explanation for the death of DA neurons in PD Bolam and Pissadaki (2012). This motivates our interest in axons that have multiple branching junctions.

Mitochondria are important for regulating physiology and cellular functions of neurons (Pekkurnaz and Wang 2022). Continuous transport of mitochondria in axons (Mogre et al. 2020) is critical for maintaining mitochondrial health. To maintain good mitochondria health in an axon, it is necessary to periodically replace either a complete mitochondrion or the proteins within it (Misgeld and Schwarz 2017).

Our specific interest is mitochondria traffic in axons with multiple branches and the effect of branched paths on mitochondrial aging (Vanhauwaert et al. 2019). Due to the large size of mitochondria, their diffusivity is negligible (Trushina 2016), and mitochondria transport is driven by molecular motors (Puttrich et al. 2022). Anterograde transport of mitochondria is driven by kinesin-1 while retrograde transport is driven by cytoplasmic dynein (Melkov and Abdu 2018; Kruppa and Buss 2021). Mitochondria can become anchored at various energy demand sites in the axon (Hollenbeck and Saxton 2005; Lees et al. 2020; Lewis et al. 2016).

Impaired mitochondrial transport in neurons plays a significant role in neurodegeneration (Sheng and Cai 2012). CNS regeneration can be promoted by turning off anchoring of mitochondria (Cheng et al. 2022). Transport of new mitochondria is essential for axon regeneration following injury (McElroy et al. 2023). We are therefore interested in the distributions of mitochondria concentration and mitochondria age in branching axons, and how these distributions are impacted by the axon geometry. We investigate how the concentration of mitochondria changes when an axon splits into two branches and how axon symmetry/asymmetry affects this concentration. We are also interested in the distribution of mitochondria mean age and age density when an axon splits into branches. Finally, we are interested in how the symmetry or asymmetry in the splitting of mitochondria flux at the branching junction affects the mean age and age density distribution of mitochondria in the branches and axon segment before the junction. The obtained results may

have implications for understanding how mitochondria aging may contribute to neurodegenerative conditions.

Karamched and Bressloff (2017) used mean-field equations to investigate transport of motor-cargo complexes to axons with multiple branches. Patel et al. (2013) developed equations for mitochondrial health, a quantity used as a proxy for mitochondrial membrane potential. Agrawal and Koslover (2021) used the mean-field theory to create models that simulated mitochondrial health as a decaying component. They applied their models to investigating the health of mitochondria in both straight and branched axons.

Kuznetsov and Kuznetsov (2022a, 2022b, 2023) developed an alternative model of mitochondria transport in an axon that is based on simulating mitochondria transport and accumulation in various energy demand sites. The motivation was to apply powerful methods developed for compartmental systems (Metzler et al. 2018; Metzler and Sierra 2018) to determine mean age and age density distributions of mitochondria in demand sites located at different distances from the soma. The model developed in our research was obtained by extending the model of mitochondria transport suggested in Kuznetsov and Kuznetsov (2022a, 2022b, 2023) to symmetric and asymmetric axons with multiple branching junctions (Fig. 1).

2. Materials and models

The transport of mitochondria in the axon is modeled using the multi-compartment model (Anderson 1983; Jacquez 1985; Jacquez and Simon 1993). This model was selected because we desired to simulate the average age and distribution of age density for mitochondria in various parts of the axon and its branches. To accomplish this, we have applied the techniques developed in Metzler et al. (2018) and Metzler and Sierra (2018), enabling particle age calculation in compartmental systems.

Intending to explore the impact of unequal length of axon branches on the age distribution of mitochondria in the axon, we represented an axon with symmetric branches by 14 demand sites (Fig. 1a) and an axon with asymmetric branches by 10 demand sites (Fig. 1b). Each demand site is composed of three separate compartments, one for anterograde mitochondria, another for stationary mitochondria, and a third for retrograde mitochondria (as illustrated in Fig. 2a,b). The mitochondria are able to transition between these compartments, and they may also move from one demand site to the next or return to the previous demand site.

Mitochondria are constantly undergoing fusion and fission. To track the mitochondria with varying lengths, a mean-field equation model was not suitable. Instead, we lumped the lengths of all the mitochondria present in a single compartment. The model thus simulates the total length of mitochondria within a compartment, as this is a conserved property. Since the axons are elongated in one direction, we characterized the mitochondrial concentration by the total length of mitochondria in a given kinetic state (anterograde, stationary, or retrograde) within a unit length of the axon. The unit of measurement for mitochondrial concentration thus is (μm of mitochondria)/μm.

In our model, the symmetric axon (Fig. 1a) has 42 compartments, each simulating 42 different mitochondrial concentrations, while the asymmetric axon (Fig. 1b) has 30 compartments, each simulating 30 different mitochondrial concentrations. In this compartmental system, time (t) is the only independent variable. The dependent variables and model parameters are summarized in Table 1 and Table 2, respectively.

Table 1. Dependent variables in the compartmental model of mitochondria transport in the axon.

Symbol	Definition	Units
l_i^a	Concentration, per unit length of the axon, of anterograde mitochondria in the compartment by the i-th demand site	(μm of mitochondria)/μm
l_i^s	Concentration, per unit length of the axon, of stationary mitochondria in the compartment by the i-th demand site	(μm of mitochondria)/μm
l_i^r	Concentration, per unit length of the axon, of retrograde mitochondria in the compartment by the i-th demand site	(μm of mitochondria)/μm
$j_{a\to b}$	Flux of mitochondria from one compartment (a) to another compartment (b), which is represented by the total length of mitochondria that are transported from compartment (a) to compartment (b) per unit of time	(μm of mitochondria) s^{-1}

Table 2. Parameters in the model of mitochondrial transport in the axon.

Symbol	Definition	Units	Value or range	Reference(s)	Value used in computations

v_a	Average velocity of anterograde mitochondria	$\mu m\, s^{-1}$	0.5	Agrawal and Koslover (2021)	0.5
v_r	Average velocity of retrograde mitochondria	$\mu m\, s^{-1}$	0.5	Agrawal and Koslover (2021)	0.5
$j_{soma \to 1}$	The production rate of mitochondria in the soma; all of these mitochondria are assumed to enter the axon	mitochondria s^{-1}	0.0375	Agrawal and Koslover (2021)	0.0375 [a]
L_{ax}	Axon length	μm	10^4 - 10^5	Agrawal and Koslover (2021)	10^4
k_w	Kinetic constant that characterizes the rate at which stationary mitochondria transition back into the motile states (anterograde and retrograde)	s^{-1}	$2\times10^{-4} - 2\times10^{-3}$ [b]	Agrawal and Koslover (2021)	5×10^{-4}
ε	A model constant that characterizes the portion of mitochondria that transition from the stationary state into the anterograde pool, while the remainder, $(1-\varepsilon)$, joins the retrograde pool		0.5	Agrawal and Koslover (2021)	0.5
f_s [c]	Fraction of mitochondria in the stationary state		0.5-0.6	Agrawal and Koslover (2021)	0.5
p_s	Probability for a motile mitochondrion to transition to a stationary state when it passes a demand site		0.4-0.5 [d]	Agrawal and Koslover (2021)	0.4
ϖ_1, ϖ_2, ϖ_3	Parameters that indicate how the mitochondrial flux splits between the upper and lower branches at the junctions (as seen in Fig. 1a,b). For instance, $\varpi_1 = 0.5$ when the flux splits evenly between both				0.5

	branches at the first branching junction.				

[a] The flux at which mitochondria synthesized in the soma enter the axon, $j_{soma\to 1}$, was estimated using the formula suggested in Agrawal and Koslover (2021), $Mv/(2L_{ax})$. The formula considers the number of mitochondria (*M*) in the axon and the average velocity of their movement (*v*). For this calculation, the value of *M* was set at 1,500 and *v* was set at 0.5 μm/s, with an axon length (L_{ax}) being set to 1 cm.

[b] To estimate k_w, we used Eq. (4) from the study conducted by Agrawal and Koslover (2021), $f_s = \frac{Nvp_s}{L_{ax}k_w + Nvp_s}$. By solving this equation for k_w and using values given in Table 2, the calculated range for k_w was found to be between 2×10^{-4} and 2×10^{-3} s^{-1} (for the number of demand sites, *N*, we used the range 10-100).

[c] Parameter f_s is not directly involved in the model; however, it is used to estimate the value of parameter k_w, as noted in footnote "b" of Table 2.

[d] The value of p_s was estimated as $p_s = \frac{N_s}{2N}$, where N_s is the average number of stops a mitochondrion makes during its back-and-forth journey in the axon (Agrawal and Koslover 2021).

2.1. Equations that express the conservation of the total length of mitochondria in various compartments for an axon with two symmetric branches (Figs. 1a and 2a)

The equation that expresses the conservation of the total length of stationary mitochondria in the most proximal demand site (# 1) is

$$L_1 \frac{dl_1^s}{dt} = p_s\left(j_{soma\to 1} + j_{2\to 1}\right) - L_1 k_w l_1^s, \tag{1}$$

where l_1^s is the concentration of stationary mitochondria in the most proximal compartment and L_1 is the length of the axonal compartments around the most proximal demand site. For axons shown in Fig. 1a and 1b, it was assumed that $L_1 = L_{ax}/6$. The lengths of all other axonal

compartments (L_2, L_3, etc.) were assumed to be the same. Also, p_s is the probability of a mobile mitochondrion transitioning to a stationary state as it passes a demand site, k_w is the kinetic constant that characterizes the rate at which stationary mitochondria reenter the mobile states (anterograde and retrograde), and $j_{soma\to 1}$ represents the rate of mitochondrial production in the soma. The fluxes between the compartments containing mobile mitochondria, $j_{a\to b}$, are given by Eqs. (43)-(70) below.

The conservation of the total length of anterograde mitochondria in the most proximal demand site (# 1) is expressed by the following equation (Fig. 2):

$$L_1 \frac{dl_1^a}{dt} = j_{soma\to 1} - p_s j_{soma\to 1} - j_{1\to 2} + \varepsilon L_1 k_w l_1^s , \tag{2}$$

where l_1^a is the concentration of anterograde mitochondria in the most proximal compartment and ε is a model constant that simulates what portion of mitochondria released from the stationary state will join the anterograde pool, with the remaining portion, $(1-\varepsilon)$, joining the retrograde pool.

The conservation of the total length of retrograde mitochondria in the most proximal demand site (# 1) is given by the following equation (Fig. 2):

$$L_1 \frac{dl_1^r}{dt} = j_{2\to 1} - p_s j_{2\to 1} - j_{1\to soma} + (1-\varepsilon) L_1 k_w l_1^s , \tag{3}$$

where l_1^a is the concentration of retrograde mitochondria in the most proximal compartment.

Stating the conservation of the total length of mitochondria in the compartments that hold stationary, anterograde, and retrograde mitochondria around other demand sites (#2, ..., 14) leads to the following equations:

$$L_2 \frac{dl_2^s}{dt} = p_s \left(j_{1\to 2} + j_{3\to 2} + j_{9\to 2} \right) - L_2 k_w l_2^s , \tag{4}$$

$$L_2 \frac{dl_2^a}{dt} = j_{1\to 2} - p_s j_{1\to 2} - j_{2\to 3} + \varepsilon L_2 k_w l_2^s , \tag{5}$$

$$L_2 \frac{dl_2^r}{dt} = j_{3\to 2} + j_{9\to 2} - p_s \left(j_{3\to 2} + j_{9\to 2} \right) - j_{2\to 1} + (1-\varepsilon) L_2 k_w l_2^s , \tag{6}$$

$$L_3 \frac{dl_3^s}{dt} = p_s \left(\varpi_1 j_{2\to3} + j_{4\to3} \right) - L_3 k_w l_3^s \,, \tag{7}$$

$$L_3 \frac{dl_3^a}{dt} = \varpi_1 j_{2\to3} - \varpi_1 p_s j_{2\to3} - j_{3\to4} + \varepsilon L_3 k_w l_3^s \,, \tag{8}$$

$$L_3 \frac{dl_3^r}{dt} = j_{4\to3} - p_s j_{4\to3} - j_{3\to2} + \left(1-\varepsilon\right) L_3 k_w l_3^s \,, \tag{9}$$

$$L_4 \frac{dl_4^s}{dt} = p_s \left(j_{3\to4} + j_{5\to4} + j_{7\to4} \right) - L_4 k_w l_4^s \,, \tag{10}$$

$$L_4 \frac{dl_4^a}{dt} = j_{3\to4} - p_s j_{3\to4} - j_{4\to5} + \varepsilon L_4 k_w l_4^s \,, \tag{11}$$

$$L_4 \frac{dl_4^r}{dt} = j_{5\to4} + j_{7\to4} - p_s \left(j_{5\to4} + j_{7\to4} \right) - j_{4\to3} + \left(1-\varepsilon\right) L_4 k_w l_4^s \,, \tag{12}$$

$$L_5 \frac{dl_5^s}{dt} = p_s \left(\varpi_2 j_{4\to5} + j_{6\to5} \right) - L_5 k_w l_5^s \,, \tag{13}$$

$$L_5 \frac{dl_5^a}{dt} = \varpi_2 j_{4\to5} - \varpi_2 p_s j_{4\to5} - j_{5\to6} + \varepsilon L_5 k_w l_5^s \,, \tag{14}$$

$$L_5 \frac{dl_5^r}{dt} = j_{6\to5} - p_s j_{6\to5} - j_{5\to4} + \left(1-\varepsilon\right) L_5 k_w l_5^s \,, \tag{15}$$

$$L_6 \frac{dl_6^s}{dt} = p_s \left(j_{5\to6} + j_{6a\to6r} \right) - L_6 k_w l_6^s \,, \tag{16}$$

$$L_6 \frac{dl_6^a}{dt} = j_{5\to6} - p_s j_{5\to6} - j_{6a\to6r} + \varepsilon L_6 k_w l_6^s \,, \tag{17}$$

$$L_6 \frac{dl_6^r}{dt} = j_{6a\to6r} - p_s j_{6a\to6r} - j_{6\to5} + \left(1-\varepsilon\right) L_6 k_w l_6^s \,, \tag{18}$$

$$L_7 \frac{dl_7^s}{dt} = p_s \left(\left(1-\varpi_2\right) j_{4\to5} + j_{8\to7} \right) - L_7 k_w l_7^s \,, \tag{19}$$

$$L_7 \frac{dl_7^a}{dt} = \left(1-\varpi_2\right) j_{4\to5} - p_s \left(1-\varpi_2\right) j_{4\to5} - j_{7\to8} + \varepsilon L_7 k_w l_7^s \,, \tag{20}$$

$$L_7 \frac{dl_7^r}{dt} = j_{8\to7} - p_s j_{8\to7} - j_{7\to4} + \left(1-\varepsilon\right) L_7 k_w l_7^s \,, \tag{21}$$

$$L_8 \frac{dl_8^s}{dt} = p_s \left(j_{7\to 8} + j_{8a\to 8r} \right) - L_8 k_w l_8^s \,, \tag{22}$$

$$L_8 \frac{dl_8^a}{dt} = j_{7\to 8} - p_s j_{7\to 8} - j_{8a\to 8r} + \varepsilon L_8 k_w l_8^s \,, \tag{23}$$

$$L_8 \frac{dl_8^r}{dt} = j_{8a\to 8r} - p_s j_{8a\to 8r} - j_{8\to 7} + \left(1-\varepsilon\right) L_8 k_w l_8^s \,, \tag{24}$$

$$L_9 \frac{dl_9^s}{dt} = \left(1-\varpi_1\right) p_s j_{2\to 3} + p_s j_{10\to 9} - L_9 k_w l_9^s \,, \tag{25}$$

$$L_9 \frac{dl_9^a}{dt} = \left(1-\varpi_1\right) j_{2\to 3} - p_s \left(1-\varpi_1\right) j_{2\to 3} - j_{9\to 10} + \varepsilon L_9 k_w l_9^s \,, \tag{26}$$

$$L_9 \frac{dl_9^r}{dt} = j_{10\to 9} - p_s j_{10\to 9} - j_{9\to 2} + \left(1-\varepsilon\right) L_9 k_w l_9^s \,, \tag{27}$$

$$L_{10} \frac{dl_{10}^s}{dt} = p_s j_{9\to 10} + p_s \left(j_{11\to 10} + j_{13\to 10} \right) - L_{10} k_w l_{10}^s \,, \tag{28}$$

$$L_{10} \frac{dl_{10}^a}{dt} = j_{9\to 10} - p_s j_{9\to 10} - j_{10\to 11} + \varepsilon L_{10} k_w l_{10}^s \,, \tag{29}$$

$$L_{10} \frac{dl_{10}^r}{dt} = j_{11\to 10} + j_{13\to 10} - p_s \left(j_{11\to 10} + j_{13\to 10} \right) - j_{10\to 9} + \left(1-\varepsilon\right) L_{10} k_w l_{10}^s \,, \tag{30}$$

$$L_{11} \frac{dl_{11}^s}{dt} = \varpi_3 p_s j_{10\to 11} + p_s j_{12\to 11} - L_{11} k_w l_{11}^s \,, \tag{31}$$

$$L_{11} \frac{dl_{11}^a}{dt} = \varpi_3 j_{10\to 11} - p_s \varpi_3 j_{10\to 11} - j_{11\to 12} + \varepsilon L_{11} k_w l_{11}^s \,, \tag{32}$$

$$L_{11} \frac{dl_{11}^r}{dt} = j_{12\to 11} - p_s j_{12\to 11} - j_{11\to 10} + \left(1-\varepsilon\right) L_{11} k_w l_{11}^s \,, \tag{33}$$

$$L_{12} \frac{dl_{12}^s}{dt} = p_s j_{11\to 12} + p_s j_{12a\to 12r} - L_{12} k_w l_{12}^s \,, \tag{34}$$

$$L_{12} \frac{dl_{12}^a}{dt} = j_{11\to 12} - p_s j_{11\to 12} - j_{12a\to 12r} + \varepsilon L_{12} k_w l_{12}^s \,, \tag{35}$$

$$L_{12} \frac{dl_{12}^r}{dt} = j_{12a\to 12r} - p_s j_{12a\to 12r} - j_{12\to 11} + \left(1-\varepsilon\right) L_{12} k_w l_{12}^s \,, \tag{36}$$

$$L_{13}\frac{dl_{13}^{s}}{dt}=\left(1-\varpi_3\right)p_s j_{10\to 11}+p_s j_{14\to 13}-L_{13}k_w l_{13}^{s}, \tag{37}$$

$$L_{13}\frac{dl_{13}^{a}}{dt}=\left(1-\varpi_3\right)j_{10\to 11}-p_s\left(1-\varpi_3\right)j_{10\to 11}-j_{13\to 14}+\varepsilon L_{13}k_w l_{13}^{s}, \tag{38}$$

$$L_{13}\frac{dl_{13}^{r}}{dt}=j_{14\to 13}-p_s j_{14\to 13}-j_{13\to 10}+\left(1-\varepsilon\right)L_{13}k_w l_{13}^{s}, \tag{39}$$

$$L_{14}\frac{dl_{14}^{s}}{dt}=p_s j_{13\to 14}+p_s j_{14a\to 14r}-L_{14}k_w l_{14}^{s}, \tag{40}$$

$$L_{14}\frac{dl_{14}^{a}}{dt}=j_{13\to 14}-p_s j_{13\to 14}-j_{14a\to 14r}+\varepsilon L_{14}k_w l_{14}^{s}, \tag{41}$$

$$L_{14}\frac{dl_{14}^{r}}{dt}=j_{14a\to 14r}-p_s j_{14a\to 14r}-j_{14\to 13}+\left(1-\varepsilon\right)L_{14}k_w l_{14}^{s}. \tag{42}$$

Eqs. (1)-(42) must be supplemented by the following equations for the mitochondrial fluxes between the demand sites. $j_{soma\to 1}$ is an input model parameter that characterizes the rate of mitochondria production in the soma (according to our model, they all enter the axon); equations for other anterograde fluxes (Fig. 2a) are

$$j_{1\to 2}=v_a l_1^a, \tag{43}$$

where v_a is the average velocity of motile mitochondria moving anterogradely.

$$j_{2\to 3}=v_a l_2^a, \tag{44}$$

$$j_{3\to 4}=v_a l_3^a, \tag{45}$$

$$j_{4\to 5}=v_a l_4^a, \tag{46}$$

$$j_{5\to 6}=v_a l_5^a, \tag{47}$$

$$j_{7\to 8}=v_a l_7^a, \tag{48}$$

$$j_{9\to 10}=v_a l_9^a, \tag{49}$$

$$j_{10\to 11}=v_a l_{10}^a, \tag{50}$$

$$j_{11\to 12}=v_a l_{11}^a, \tag{51}$$

$$j_{13\to14} = v_a l_{13}^a . \tag{52}$$

Equations for retrograde fluxes (Fig. 2) are

$$j_{1\to soma} = v_r l_1^r , \tag{53}$$

where v_r is the average velocity of motile mitochondria that are moving retrogradely.

$$j_{2\to1} = v_r l_2^r , \tag{54}$$

$$j_{3\to2} = v_r l_3^r , \tag{55}$$

$$j_{4\to3} = v_r l_4^r , \tag{56}$$

$$j_{5\to4} = v_r l_5^r , \tag{57}$$

$$j_{6\to5} = v_r l_6^r , \tag{58}$$

$$j_{7\to4} = v_r l_7^r , \tag{59}$$

$$j_{8\to7} = v_r l_8^r , \tag{60}$$

$$j_{9\to2} = v_r l_9^r , \tag{61}$$

$$j_{10\to9} = v_r l_{10}^r , \tag{62}$$

$$j_{11\to10} = v_r l_{11}^r , \tag{63}$$

$$j_{12\to11} = v_r l_{12}^r , \tag{64}$$

$$j_{13\to10} = v_r l_{13}^r , \tag{65}$$

$$j_{14\to13} = v_r l_{14}^r . \tag{66}$$

The turn-around fluxes (Fig. 2) are simulated by the following equations:

$$j_{6a\to6r} = v_a l_6^a , \tag{67}$$

$$j_{8a\to8r} = v_a l_8^a , \tag{68}$$

$$j_{12a\to12r} = v_a l_{12}^a , \tag{69}$$

$$j_{14a\to14r} = v_a l_{14}^a . \tag{70}$$

2.2. Model of mean age and age density distributions of mitochondria in the demand sites for the symmetric axon displayed in Figs. 1a and 2a

To compute the age density distributions of mitochondria in the stationary and moving states in the compartments surrounding the demand sites, the method described in Metzler et al. (2018) and Metzler and Sierra (2018) was utilized. To apply the techniques developed in these papers, equations (1)-(42) were recast into the following matrix equation:

$$\frac{d}{dt}\mathbf{C}^*(t) = \mathrm{B}\left(\mathbf{C}^*(t), t\right)\mathbf{C}^*(t) + \mathbf{u}(t), \tag{71}$$

where $\mathbf{C}^*$ is referred to as a state vector (using the terminology of Metzler et al. (2018)). $\mathbf{C}^*$ is defined by its components:

$$C_1^* = l_1 L_1, \ldots, C_N^* = l_N L_N, C_{N+1}^* = l_1^a L_1, \ldots, C_{2N-1}^* = l_{N-1}^a L_{N-1}, C_{2N}^* = l_N^m L_N, C_{2N+1}^* = l_1^r L_1, C_{3N-1}^* = l_{N-1}^r L_{N-1}, \tag{72}$$

In Eq. (72)

$$\hat{l}_1 = l_1, \ldots, \hat{l}_N = l_N, \hat{l}_{N+1} = l_1^a, \ldots, \hat{l}_{2N-1} = l_{N-1}^a, \hat{l}_{2N} = l_N^m, \hat{l}_{2N+1} = l_1^r, \hat{l}_{3N} = l_N^r. \tag{73}$$

For the axon shown in Figure 1a, there are 14 demand sites (N=14). Although the governing equations (1)-(42) are easier to interpret in terms of the concentration of mitochondria in a compartment, to make further progress, they need to be re-scaled in the form given by Eqs. (71) and (72). This is because the conserved quantity is the total length of mitochondria in a compartment, not its linear density (concentration). Re-stating the governing equations in the form of Eqs. (71) and (72) enables the utilization of the methods developed in Metzler et al. (2018) and Metzler and Sierra (2018) for computing the mean age and age density distributions of mitochondria in various compartments.

The total length of mitochondria in stationary states is represented by the first N components of the state vector, the total length of mitochondria in anterograde states is represented by the next N components (N+1,…,2N), and the total length of mitochondria in retrograde states is represented by the last N components (2N+1,…,3N), see Fig. 2a. Vector $\mathbf{u}(t)$ is defined below by Eqs. (202) and (203).

We accounted for the internal mitochondria fluxes between the compartments, the external mitochondria flux entering the terminal from the axon, and the mitochondria flux leaving the

terminal to move back to the axon (Fig. 2a). Equations for the following elements of matrix B defined in Eq. (71) were obtained by analyzing mitochondria fluxes to and from the compartments surrounding the most proximal demand site.

$$b_{1,1} = -L_1 k_w l_1^s / \left(L_1 l_1^s \right), \tag{74}$$

$$b_{N+1,N+1} = -\left(p_s j_{soma \to 1} + j_{1 \to 2} \right) / \left(L_1 l_1^a \right), \tag{75}$$

$$b_{2N+1,2N+1} = -\left(p_s j_{2 \to 1} + j_{1 \to soma} \right) / \left(L_1 l_1^r \right), \tag{76}$$

$$b_{N+1,1} = \varepsilon L_1 k_w l_1^s / \left(L_1 l_1^s \right), \tag{77}$$

$$b_{1,N+1} = p_s j_{soma \to 1} / \left(L_1 l_1^a \right), \tag{78}$$

$$b_{2N+1,1} = \left(1 - \varepsilon \right) L_1 k_w l_1^s / \left(L_1 l_1^s \right), \tag{79}$$

$$b_{1,2N+1} = p_s j_{2 \to 1} / \left(L_1 l_1^r \right), \tag{80}$$

$$b_{N+2,N+1} = j_{1 \to 2} / \left(L_1 l_1^a \right), \tag{81}$$

$$b_{2N+1,2N+2} = j_{2 \to 1} / \left(L_2 l_2^r \right), \tag{82}$$

$$b_{2,2} = -L_2 k_w l_2^s / \left(L_2 l_2^s \right). \tag{83}$$

For other demand sites:

$$b_{N+2,N+2} = -\left(p_s j_{1 \to 2} + j_{2 \to 3} \right) / \left(L_2 l_2^a \right), \tag{84}$$

$$b_{2N+2,2N+2} = -\left(p_s j_{3 \to 2} + p_s j_{9 \to 2} + j_{2 \to 1} \right) / \left(L_2 l_2^r \right), \tag{85}$$

$$b_{N+2,2} = \varepsilon L_2 k_w l_2^s / \left(L_2 l_2^s \right), \tag{86}$$

$$b_{2,N+2} = p_s j_{1 \to 2} / \left(L_2 l_2^a \right), \tag{87}$$

$$b_{2N+2,2} = \left(1 - \varepsilon \right) L_2 k_w l_2^s / \left(L_2 l_2^s \right), \tag{88}$$

$$b_{2,2N+2} = p_s \left(j_{3 \to 2} + j_{9 \to 2} \right) / \left(L_2 l_2^r \right), \tag{89}$$

$$b_{N+9,N+2} = \left(1-\varpi_1\right) j_{2\to 3} / \left(L_2 l_2^a\right), \tag{90}$$

$$b_{N+3,N+2} = \varpi_1 j_{2\to 3} / \left(L_2 l_2^a\right), \tag{91}$$

$$b_{3,3} = -L_3 k_w l_3^s / \left(L_3 l_3^s\right), \tag{92}$$

$$b_{N+3,N+3} = -\left(\varpi_1 p_s j_{2\to 3} + j_{3\to 4}\right) / \left(L_3 l_3^a\right), \tag{93}$$

$$b_{2N+3,2N+3} = -\left(p_s j_{4\to 3} + j_{3\to 2}\right) / \left(L_3 l_3^r\right), \tag{94}$$

$$b_{N+3,3} = \varepsilon L_3 k_w l_3^s / \left(L_3 l_3^s\right), \tag{95}$$

$$b_{3,N+3} = \varpi_1 p_s j_{2\to 3} / \left(L_3 l_3^a\right), \tag{96}$$

$$b_{2N+3,3} = \left(1-\varepsilon\right) L_3 k_w l_3^s / \left(L_3 l_3^s\right), \tag{97}$$

$$b_{3,2N+3} = p_s j_{4\to 3} / \left(L_3 l_3^r\right), \tag{98}$$

$$b_{N+4,N+3} = j_{3\to 4} / \left(L_3 l_3^a\right), \tag{99}$$

$$b_{4,N+4} = p_s j_{3\to 4} / \left(L_4 l_4^a\right), \tag{100}$$

$$b_{4,4} = -L_4 k_w l_4^s / \left(L_4 l_4^s\right), \tag{101}$$

$$b_{N+4,N+4} = -\left(p_s j_{3\to 4} + j_{4\to 5}\right) / \left(L_4 l_4^a\right), \tag{102}$$

$$b_{N+5,N+4} = \varpi_2 j_{4\to 5} / \left(L_4 l_4^a\right), \tag{103}$$

$$b_{N+7,N+4} = \left(1-\varpi_2\right) j_{4\to 5} / \left(L_4 l_4^a\right), \tag{104}$$

$$b_{2N+4,2N+4} = -\left(p_s j_{5\to 4} + p_s j_{7\to 4} + j_{4\to 3}\right) / \left(L_4 l_4^r\right), \tag{105}$$

$$b_{N+4,4} = \varepsilon L_4 k_w l_4^s / \left(L_4 l_4^s\right), \tag{106}$$

$$b_{2N+4,4} = \left(1-\varepsilon\right) L_4 k_w l_4^s / \left(L_4 l_4^s\right), \tag{107}$$

$$b_{4,2N+4} = p_s \left(j_{5\to 4} + j_{7\to 4}\right) / \left(L_4 l_4^r\right), \tag{108}$$

$$b_{2N+3,2N+4} = j_{4\to 3} / \left(L_4 l_4^r \right), \tag{109}$$

$$b_{2N+2,2N+3} = j_{3\to 2} / \left(L_3 l_3^r \right), \tag{110}$$

$$b_{N+6,N+5} = j_{5\to 6} / \left(L_5 l_5^a \right), \tag{111}$$

$$b_{5,5} = -L_5 k_w l_5^s / \left(L_5 l_5^s \right), \tag{112}$$

$$b_{N+5,N+5} = -\left(\varpi_2 p_s j_{4\to 5} + j_{5\to 6} \right) / \left(L_5 l_5^a \right), \tag{113}$$

$$b_{2N+5,2N+5} = -\left(p_s j_{6\to 5} + j_{5\to 4} \right) / \left(L_5 l_5^r \right), \tag{114}$$

$$b_{2N+4,2N+5} = j_{5\to 4} / \left(L_5 l_5^r \right), \tag{115}$$

$$b_{N+5,5} = \varepsilon L_5 k_w l_5^s / \left(L_5 l_5^s \right), \tag{116}$$

$$b_{5,N+5} = \varpi_2 p_s j_{4\to 5} / \left(L_5 l_5^a \right), \tag{117}$$

$$b_{2N+5,5} = \left(1-\varepsilon \right) L_5 k_w l_5^s / \left(L_5 l_5^s \right), \tag{118}$$

$$b_{5,2N+5} = p_s j_{6\to 5} / \left(L_5 l_5^r \right), \tag{119}$$

$$b_{6,N+6} = p_s j_{5\to 6} / \left(L_6 l_6^a \right), \tag{120}$$

$$b_{6,6} = -L_6 k_w l_6^s / \left(L_6 l_6^s \right), \tag{121}$$

$$b_{N+6,N+6} = -\left(p_s j_{5\to 6} + j_{6a\to 6r} \right) / \left(L_6 l_6^a \right), \tag{122}$$

$$b_{2N+6,2N+6} = -\left(p_s j_{6a\to 6r} + j_{6\to 5} \right) / \left(L_6 l_6^r \right), \tag{123}$$

$$b_{N+6,6} = \varepsilon L_6 k_w l_6^s / \left(L_6 l_6^s \right), \tag{124}$$

$$b_{6,2N+6} = p_s j_{6a\to 6r} / \left(L_6 l_6^r \right), \tag{125}$$

$$b_{2N+6,6} = \left(1-\varepsilon \right) L_6 k_w l_6^s / \left(L_6 l_6^s \right), \tag{126}$$

$$b_{2N+5,2N+6} = j_{6\to 5} / \left(L_6 l_6^r \right), \tag{127}$$

$$b_{2N+6,N+6} = j_{6a\to 6r} / \left(L_6 l_6^a \right), \tag{128}$$

$$b_{7,N+7} = \left(1-\varpi_2\right) p_s j_{4\to 5} / \left(L_7 l_7^a \right), \tag{129}$$

$$b_{7,7} = -L_7 k_w l_7^s / \left(L_7 l_7^s \right), \tag{130}$$

$$b_{N+7,N+7} = -\left(\left(1-\varpi_2\right) p_s j_{4\to 5} + j_{7\to 8} \right) / \left(L_7 l_7^a \right), \tag{131}$$

$$b_{N+8,N+7} = j_{7\to 8} / \left(L_7 l_7^a \right), \tag{132}$$

$$b_{2N+7,2N+7} = -\left(p_s j_{8\to 7} + j_{7\to 4} \right) / \left(L_7 l_7^r \right), \tag{133}$$

$$b_{7,2N+7} = p_s j_{8\to 7} / \left(L_7 l_7^r \right), \tag{134}$$

$$b_{N+7,7} = \varepsilon L_7 k_w l_7^s / \left(L_7 l_7^s \right), \tag{135}$$

$$b_{2N+7,7} = \left(1-\varepsilon\right) L_7 k_w l_7^s / \left(L_7 l_7^s \right), \tag{136}$$

$$b_{2N+4,2N+7} = j_{7\to 4} / \left(L_7 l_7^r \right), \tag{137}$$

$$b_{8,N+8} = p_s j_{7\to 8} / \left(L_8 l_8^a \right), \tag{138}$$

$$b_{8,8} = -L_8 k_w l_8^s / \left(L_8 l_8^s \right), \tag{139}$$

$$b_{N+8,N+8} = -\left(p_s j_{7\to 8} + j_{8a\to 8r} \right) / \left(L_8 l_8^a \right), \tag{140}$$

$$b_{2N+8,2N+8} = -\left(p_s j_{8a\to 8r} + j_{8\to 7} \right) / \left(L_8 l_8^r \right), \tag{141}$$

$$b_{8,2N+8} = p_s j_{8a\to 8r} / \left(L_8 l_8^r \right), \tag{142}$$

$$b_{2N+7,2N+8} = j_{8\to 7} / \left(L_8 l_8^r \right), \tag{143}$$

$$b_{N+8,8} = \varepsilon L_8 k_w l_8^s / \left(L_8 l_8^s \right), \tag{144}$$

$$b_{2N+8,8} = \left(1-\varepsilon\right) L_8 k_w l_8^s / \left(L_8 l_8^s \right), \tag{145}$$

$$b_{2N+8,N+8} = j_{8a\to 8r} / \left(L_8 l_8^a \right), \tag{146}$$

$$b_{9,N+9} = \left(1-\varpi_1\right) p_s j_{2\to 3} / \left(L_9 l_9^a\right), \tag{147}$$

$$b_{9,9} = -L_9 k_w l_9^s / \left(L_9 l_9^s\right), \tag{148}$$

$$b_{N+9,N+9} = -\left(\left(1-\varpi_1\right) p_s j_{2\to 3} + j_{9\to 10}\right) / \left(L_9 l_9^a\right), \tag{149}$$

$$b_{2N+9,2N+9} = -\left(p_s j_{10\to 9} + j_{9\to 2}\right) / \left(L_9 l_9^r\right), \tag{150}$$

$$b_{2N+2,2N+9} = j_{9\to 2} / \left(L_9 l_9^r\right), \tag{151}$$

$$b_{N+9,9} = \varepsilon L_9 k_w l_9^s / \left(L_9 l_9^s\right), \tag{152}$$

$$b_{2N+9,9} = \left(1-\varepsilon\right) L_9 k_w l_9^s / \left(L_9 l_9^s\right), \tag{153}$$

$$b_{9,2N+9} = p_s j_{10\to 9} / \left(L_9 l_9^r\right), \tag{154}$$

$$b_{N+10,N+9} = j_{9\to 10} / \left(L_9 l_9^a\right), \tag{155}$$

$$b_{10,N+10} = p_s j_{9\to 10} / \left(L_{10} l_{10}^a\right), \tag{156}$$

$$b_{10,10} = -L_{10} k_w l_{10}^s / \left(L_{10} l_{10}^s\right), \tag{157}$$

$$b_{N+10,N+10} = -\left(p_s j_{9\to 10} + j_{10\to 11}\right) / \left(L_{10} l_{10}^a\right), \tag{158}$$

$$b_{2N+10,2N+10} = -\left(p_s \left(j_{11\to 10} + j_{13\to 10}\right) + j_{10\to 9}\right) / \left(L_{10} l_{10}^r\right), \tag{159}$$

$$b_{2N+9,2N+10} = j_{10\to 9} / \left(L_{10} l_{10}^r\right), \tag{160}$$

$$b_{N+10,10} = \varepsilon L_{10} k_w l_{10}^s / \left(L_{10} l_{10}^s\right), \tag{161}$$

$$b_{2N+10,10} = \left(1-\varepsilon\right) L_{10} k_w l_{10}^s / \left(L_{10} l_{10}^s\right), \tag{162}$$

$$b_{10,2N+10} = p_s \left(j_{11\to 10} + j_{13\to 10}\right) / \left(L_{10} l_{10}^r\right), \tag{163}$$

$$b_{N+11,N+10} = \varpi_3 j_{10\to 11} / \left(L_{10} l_{10}^a\right), \tag{164}$$

$$b_{N+13,N+10} = \left(1-\varpi_3\right) j_{10\to 11} / \left(L_{10} l_{10}^a\right), \tag{165}$$

$$b_{11,N+11} = \varpi_3 p_s j_{10\to 11} / \left(L_{11} l_{11}^a \right), \tag{166}$$

$$b_{11,11} = -L_{11} k_w l_{11}^s / \left(L_{11} l_{11}^s \right), \tag{167}$$

$$b_{N+11,N+11} = -\left(\varpi_3 p_s j_{10\to 11} + j_{11\to 12} \right) / \left(L_{11} l_{11}^a \right), \tag{168}$$

$$b_{2N+11,2N+11} = -\left(p_s j_{12\to 11} + j_{11\to 10} \right) / \left(L_{11} l_{11}^r \right), \tag{169}$$

$$b_{2N+10,2N+11} = j_{11\to 10} / \left(L_{11} l_{11}^r \right), \tag{170}$$

$$b_{N+11,11} = \varepsilon L_{11} k_w l_{11}^s / \left(L_{11} l_{11}^s \right), \tag{171}$$

$$b_{2N+11,11} = \left(1-\varepsilon \right) L_{11} k_w l_{11}^s / \left(L_{11} l_{11}^s \right), \tag{172}$$

$$b_{11,2N+11} = p_s j_{12\to 11} / \left(L_{11} l_{11}^r \right), \tag{173}$$

$$b_{N+12,N+11} = j_{11\to 12} / \left(L_{11} l_{11}^a \right), \tag{174}$$

$$b_{12,N+12} = p_s j_{11\to 12} / \left(L_{12} l_{12}^a \right), \tag{175}$$

$$b_{12,12} = -L_{12} k_w l_{12}^s / \left(L_{12} l_{12}^s \right), \tag{176}$$

$$b_{N+12,N+12} = -\left(p_s j_{11\to 12} + j_{12a\to 12r} \right) / \left(L_{12} l_{12}^a \right), \tag{177}$$

$$b_{2N+12,2N+12} = -\left(p_s j_{12a\to 12r} + j_{12\to 11} \right) / \left(L_{12} l_{12}^r \right), \tag{178}$$

$$b_{2N+11,2N+12} = j_{12\to 11} / \left(L_{12} l_{12}^r \right), \tag{179}$$

$$b_{N+12,12} = \varepsilon L_{12} k_w l_{12}^s / \left(L_{12} l_{12}^s \right), \tag{180}$$

$$b_{2N+12,12} = \left(1-\varepsilon \right) L_{12} k_w l_{12}^s / \left(L_{12} l_{12}^s \right), \tag{181}$$

$$b_{12,2N+12} = p_s j_{12a\to 12r} / \left(L_{12} l_{12}^r \right), \tag{182}$$

$$b_{2N+12,N+12} = j_{12a\to 12r} / \left(L_{12} l_{12}^a \right), \tag{183}$$

$$b_{13,N+13} = \left(1-\varpi_3 \right) p_s j_{10\to 11} / \left(L_{13} l_{13}^a \right), \tag{184}$$

$$b_{13,13} = -L_{13}k_w l_{13}^s / \left(L_{13}l_{13}^s\right), \tag{185}$$

$$b_{N+13,N+13} = -\left(\left(1-\varpi_3\right)p_s j_{10\to 11} + j_{13\to 14}\right) / \left(L_{13}l_{13}^a\right), \tag{186}$$

$$b_{2N+13,2N+13} = -\left(p_s j_{14\to 13} + j_{13\to 10}\right) / \left(L_{13}l_{13}^r\right), \tag{187}$$

$$b_{2N+10,2N+13} = j_{13\to 10} / \left(L_{13}l_{13}^r\right), \tag{188}$$

$$b_{N+13,13} = \varepsilon L_{13}k_w l_{13}^s / \left(L_{13}l_{13}^s\right), \tag{189}$$

$$b_{2N+13,13} = \left(1-\varepsilon\right)L_{13}k_w l_{13}^s / \left(L_{13}l_{13}^s\right), \tag{190}$$

$$b_{13,2N+13} = p_s j_{14\to 13} / \left(L_{13}l_{13}^r\right), \tag{191}$$

$$b_{N+14,N+13} = j_{13\to 14} / \left(L_{13}l_{13}^a\right), \tag{192}$$

$$b_{14,N+14} = p_s j_{13\to 14} / \left(L_{14}l_{14}^a\right), \tag{193}$$

$$b_{14,14} = -L_{14}k_w l_{14}^s / \left(L_{14}l_{14}^s\right), \tag{194}$$

$$b_{N+14,N+14} = -\left(p_s j_{13\to 14} + j_{14a\to 14b}\right) / \left(L_{14}l_{14}^a\right), \tag{195}$$

$$b_{2N+14,2N+14} = -\left(p_s j_{14a\to 14b} + j_{14\to 13}\right) / \left(L_{14}l_{14}^r\right), \tag{196}$$

$$b_{N+14,14} = \varepsilon L_{14}k_w l_{14}^s / \left(L_{14}l_{14}^s\right), \tag{197}$$

$$b_{2N+14,14} = \left(1-\varepsilon\right)L_{14}k_w l_{14}^s / \left(L_{14}l_{14}^s\right), \tag{198}$$

$$b_{14,2N+14} = p_s j_{14a\to 14b} / \left(L_{14}l_{14}^r\right), \tag{199}$$

$$b_{2N+14,N+14} = j_{14a\to 14r} / \left(L_{14}l_{14}^a\right), \tag{200}$$

$$b_{2N+13,2N+14} = j_{14\to 13} / \left(L_{14}l_{14}^r\right). \tag{201}$$

All other elements of matrix B, apart from those given by Eqs. (74)-(201), are equal to zero. When considering a single mitochondrion in the axon (its behavior is independent of all other mitochondria), the elements on the main diagonal determine the length of time it remains in a

given compartment, while the off-diagonal elements describe the probabilities of it transitioning to other compartments (Metzler and Sierra 2018).

The only flux entering the axon is the anterograde flux from the soma to the compartment with anterograde mitochondria by the most proximal demand site, $j_{soma\to 1}$. Our model assumes that any mitochondria leaving the axon (their flux is $j_{1\to soma}$) are degraded in the soma and not re-entering the axon. We also assume that all mitochondria entering the axon (their flux is $j_{soma\to 1}$) are newly synthesized in the soma and have an age of zero at the time of entry. The mitochondrial age is calculated as the time since the mitochondria entered the axon.

The following equation yields the $(N+1)^{\text{th}}$ element of vector **u**:

$$u_{N+1} = j_{soma\to 1}\,. \tag{202}$$

As no other external fluxes enter the terminal,

$$u_i = 0 \quad (i=1,\ldots,N,N+2,\ldots,N+6,2N+1,\ldots,2N+14). \tag{203}$$

2.3. Calculating the mean age and age density distribution of mitochondria

A steady state solution for Eq. (71) can be obtained as follows (Table 1 of Metzler and Sierra 2018):

$$\mathbf{C}^*_{ss} = -\mathrm{B}^{-1}_{ss}\mathbf{u}_{ss}\,, \tag{204}$$

where the superscript -1 on a matrix denotes the inverse of the matrix, while the subscript *ss* stands for steady state. The mean ages of mitochondria in various compartments displayed in Fig. 2a at steady state can be calculated as follows:

$$\overline{\mathbf{c}}_{ss} = -\left(\hat{\mathbf{C}}^*_{ss}\right)^{-1}\mathrm{B}^{-1}_{ss}\mathbf{C}^*_{ss}\,. \tag{205}$$

In Eq. (205)

$$\hat{\mathbf{C}}^*_{ss} = \mathrm{diag}\left(C^*_{1,ss}, C^*_{2,ss}, \ldots, C^*_{3N,ss}\right) \tag{206}$$

is the diagonal matrix with the components of the state vector, which is defined in Eq. (72), on the main diagonal. These components ($C^*_{1,ss}$, $C^*_{2,ss}$, etc.) are determined at the steady state. Furthermore, in Eq. (205)

$$\overline{\mathbf{c}}_{ss} = \left(\overline{c}_{1,ss},\ldots,\overline{c}_{3N,ss}\right)^T \tag{207}$$

represents a column vector composed of the mean ages of mitochondria in various compartments (superscript T means transposed).

The vector whose components represent the age density of mitochondria residing in various compartments at steady state can be calculated as follows:

$$\mathbf{p}_{ss}\left(c\right) = \left(\hat{\mathbf{C}}^*_{ss}\right)^{-1} \mathrm{e}^{c\mathrm{B}_{ss}} \mathbf{u}_{ss}\,, \tag{208}$$

where e denotes the matrix exponential. The age density of mitochondria can be defined as the portion of mitochondria that have an age within a specific interval, T and T+dT, throughout dT. The total number of mitochondria in a particular kinetic state can be obtained by integrating the age density of mitochondria from 0 to infinity. Additionally, integrating over any time interval will yield the number of mitochondria that fall within that time interval.

Governing equations for the case of an axon with two asymmetric branches (Figs. 1b and 2b) are given in section S1 in Supplemental Materials.

2.4. Numerical solution procedure

In this paper, we utilized two different methods for computing the steady state distributions of mitochondria in the axon. The two methods were used to validate each other. The first method involves solving the transient equations until the numerical solutions reach a steady state. Since we are only interested in the solution at steady state, we can choose any initial condition (for simplicity, we used the zero boundary condition). Eqs. (1)-(42), which simulate the transport of mitochondria in the axon with two branches of equal length (as shown in Fig. 1a), were solved using the MATLAB solver ODE45 (MATLAB R2020b, MathWorks, Natick, MA, USA).

Eqs. (204)-(208) allow us to find steady state solutions directly. We implemented these equations using standard MATLAB operators, such as matrix inverse and matrix exponential.

3. Results

The calculations in this paper are performed for the axons depicted in Fig. 1a and 1b, considering the scenario where the flow of mitochondria is divided equally at each branching junction ($\varpi_1 = \varpi_2 = \varpi_3 = 0.5$ for the axon depicted in Fig. 1a and $\varpi_1 = \varpi_2 = 0.5$ for the axon depicted in

Fig. 1b). As a result, the concentration of mitochondria decreases by half at each branching junction (Figs. 3a and 3b). This is due to the decrease in the rate of flow of mitochondria, which is proportional to the concentration of mitochondria (as described in Eqs. (43)-(70) and (S31)-(S50)). Note that the effect of mitophagy was neglected.

The mean age of anterogradely moving mitochondria in the symmetric (Fig. 1a) and asymmetric (Fig. 1b) axons increases from the most proximal (#1) to the most distal (#6) demand site, i.e. $1 \to 2 \to 3 \to 4 \to 5 \to 6$ (Fig. 4). This is because the mitochondria get older as they move from one demand site to the next (see the age density distributions displayed in Figs. S1-S6). The same holds true for stationary mitochondria. The pattern for retrograde mitochondria is more complicated, as two opposing trends shape their distribution: (i) they get older as they move from the more proximal to the more distal demand site, and (ii) there is a transfer of newer mitochondria from stationary states (Fig. 2a,b). Fig. 4 shows that in the asymmetric axon (Fig. 1b), the average age of mitochondria is lower due to its shorter total branch length compared to the symmetric axon (Fig. 1a).

The ages of mitochondria displayed in Fig. 4 are comparable with the estimate reported in Kuznetsov and Kuznetsov (2022a) (22 hours). Kuznetsov and Kuznetsov (2022a) estimated the mean age of mitochondria using experimental data reported in Ferree et al. (2013). The results in Fig. 4 are also consistent with Mandal et al. (2021), which reported that the complete turnover of axon terminal mitochondria in zebrafish neurons occurs within 24 h.

The average age of mitochondria does not provide a comprehensive understanding of the age of mitochondria within the axon. Each demand site contains mitochondria of different ages, as illustrated by the mitochondrial age density distributions in symmetric (Figs. S1-S3) and asymmetric (Figs. S4-S6) axons. The presence of long tails suggests that each demand site contains mitochondria that are significantly older than the mean age.

The newly formed anterograde mitochondria with a zero-age are delivered to the anterograde compartment at the most proximal demand site (#1). This is why the highest concentration of anterograde mitochondria is found at zero-age at the most proximal demand site (Fig. 5a). As the demand sites get farther away from the soma, the peak of the age density distribution for anterograde mitochondria shifts towards older mitochondria (Fig. 5a). The age density distributions of mitochondria in demand sites 8 and 14 in the axon shown in Fig. 1a are the same due to symmetry (Figs. 5b, 6b, and 7b). However, the age density distribution at demand site 10 is smaller due to its proximity to the soma compared to demand site 8 (Fig. 1a, 1b).

The difference between the age density of anterograde mitochondria in symmetric and asymmetric axons is not very visible (Fig. 5). The difference in mean ages seen in Fig. 4 primarily results from the skewed right shape of the age density distributions and longer tails in the positive direction for the symmetrical axon. This indicates a higher number of older mitochondria in the symmetric axon (Metzler and Sierra 2018). This is because the symmetric axon (Fig. 1a) has longer branches than the asymmetric axon (Fig. 1b), which leads to a longer travel time for retrograde mitochondria. However, the difference between the age density distributions in symmetric and asymmetric axons becomes more pronounced for stationary mitochondria (compare the age density distributions for demand site 1 in Fig. 6a) and particularly for retrograde mitochondria (compare the age density distributions for demand site 1 in Fig. 7a).

4. Discussion, limitations of the model, and future directions

The average total length of dopaminergic neurons in rats is around 0.5 meters (Matsuda et al. 2009), which roughly corresponds to a neuron with 14 branching levels (Pissadaki and Bolam 2013). Our findings in this paper demonstrate the mitochondrial concentration decreases by half when the mitochondrial flux splits in half at each branching junction. This aligns with previous research indicating that the density of mitochondria is evenly divided at each branching junction (Agrawal and Koslover 2021). As a result, the mitochondrial concentration in the most distal branch is reduced by $2^{14-1} = 8192$ times compared to the most proximal branch. The ATP concentration in axons is estimated to be between 2-4 mM Pathak et al. (2015), and a minimum ATP concentration of 0.8 mM is needed in boutons to sustain synaptic transmission Pathak et al. (2015). However, based on our findings, the ATP concentration in the most distal branch would be much lower at $(2-4)\,\text{mM} / 8192 = (2.44 - 4.88) \times 10^{-4}\,\text{mM}$, which is far below the minimum required (0.8 mM). Further investigation is necessary to understand how dopaminergic neurons can maintain ATP concentration to sustain transmission in distal boutons.

Acknowledgment

IAK acknowledges the fellowship support of the Paul and Daisy Soros Fellowship for New Americans and the NIH/National Institute of Mental Health (NIMH) Ruth L. Kirchstein NRSA (F30 MH122076-01). AVK acknowledges the support of the National Science Foundation (award

CBET-2042834) and the Alexander von Humboldt Foundation through the Humboldt Research Award.

References

Agrawal, A. and Koslover, E.F., Optimizing mitochondrial maintenance in extended neuronal projections, PLOS Computational Biology, vol. 17, pp. e1009073, 2021.

Bolam, J.P. and Pissadaki, E.K., Living on the edge with too many mouths to feed: Why dopamine neurons die, Movement Disorders, vol. 27, pp. 1478-1483, 2012.

Cheng, X., Huang, N., and Sheng, Z., Programming axonal mitochondrial maintenance and bioenergetics in neurodegeneration and regeneration, Neuron, vol. 110, pp. 1899-1923, 2022.

Chinta, S. and Andersen, J., Dopaminergic neurons, International Journal of Biochemistry & Cell Biology, vol. 37, pp. 942-946, 2005.

Ferree, A.W., Trudeau, K., Zik, E., Benador, I.Y., Twig, G., Gottlieb, R.A., and Shirihai, O.S., MitoTimer probe reveals the impact of autophagy, fusion, and motility on subcellular distribution of young and old mitochondrial protein and on relative mitochondrial protein age, Autophagy, vol. 9, pp. 1887-1896, 2013.

Guo, J., Zhao, X., Li, Y., Li, G., and Liu, X., Damage to dopaminergic neurons by oxidative stress in Parkinson's disease (Review), International Journal of Molecular Medicine, vol. 41, pp. 1817-1825, 2018.

Hollenbeck, P.J. and Saxton, W.M., The axonal transport of mitochondria, Journal of Cell Science, vol. 118, pp. 5411-5419, 2005.

Karamched, B.R. and Bressloff, P.C., Effects of cell geometry on reversible vesicular transport, Journal of Physics A-Mathematical and Theoretical, vol. 50, pp. 055601, 2017.

Kruppa, A.J. and Buss, F., Motor proteins at the mitochondria cytoskeleton interface, Journal of Cell Science, vol. 134, pp. jcs226084, 2021.

Kuznetsov, I.A. and Kuznetsov, A.V., Effect of mitochondrial circulation on mitochondrial age density distribution, bioRxiv, https://biorxiv.org/cgi/content/short/2022.12.01.518783, 2023.

Kuznetsov, I.A. and Kuznetsov, A., V., Computation of the mitochondrial age distribution along the axon length, Computer Methods in Biomechanics and Biomedical Engineering, pp. https://doi.org/10.1080/10255842.2022.2128784, 2022a.

Kuznetsov, I.A. and Kuznetsov, A., V., Effects of axon branching and asymmetry between the branches on transport, mean age, and age density distributions of mitochondria in neurons: A computational study, International Journal for Numerical Methods in Biomedical Engineering, vol. 38, pp. e3648, 2022b.

Lees, R.M., Johnson, J.D., and Ashby, M.C., Presynaptic Boutons That Contain Mitochondria Are More Stable, Frontiers in Synaptic Neuroscience, vol. 11, pp. 37, 2020.

Lewis, T.L., Jr., Turi, G.F., Kwon, S., Losonczy, A., and Polleux, F., Progressive Decrease of Mitochondrial Motility during Maturation of Cortical Axons In Vitro and In Vivo, Current Biology, vol. 26, pp. 2602-2608, 2016.

Mandal, A., Wong, H.C., Pinter, K., Mosqueda, N., Beirl, A., Lomash, R.M., Won, S., Kindt, K.S., and Drerup, C.M., Retrograde Mitochondrial Transport Is Essential for Organelle Distribution and Health in Zebrafish Neurons, Journal of Neuroscience, vol. 41, pp. 1371-1392, 2021.

Matsuda, W., Furuta, T., Nakamura, K.C., Hioki, H., Fujiyama, F., Arai, R., and Kaneko, T., Single Nigrostriatal Dopaminergic Neurons Form Widely Spread and Highly Dense Axonal Arborizations in the Neostriatum, Journal of Neuroscience, vol. 29, pp. 444-453, 2009.

McElroy, T., Zeidan, R.S., Rathor, L., Han, S.M., and Xiao, R., The role of mitochondria in the recovery of neurons after injury, Neural Regeneration Research, vol. 18, pp. 317-318, 2023.

Melkov, A. and Abdu, U., Regulation of long-distance transport of mitochondria along microtubules, Cellular and Molecular Life Sciences, vol. 75, pp. 163-176, 2018.

Metzler, H., Muller, M., and Sierra, C.A., Transit-time and age distributions for nonlinear time-dependent compartmental systems, Proceedings of the National Academy of Sciences of the United States of America, vol. 115, pp. 1150-1155, 2018.

Metzler, H. and Sierra, C.A., Linear Autonomous Compartmental Models as Continuous-Time Markov Chains: Transit-Time and Age Distributions, Mathematical Geosciences, vol. 50, pp. 1-34, 2018.

Misgeld, T. and Schwarz, T.L., Mitostasis in Neurons: Maintaining Mitochondria in an Extended Cellular Architecture, Neuron, vol. 96, pp. 651-666, 2017.

Mogre, S.S., Brown, A., I., and Koslover, E.F., Getting around the cell: physical transport in the intracellular world, Physical Biology, vol. 17, pp. 061003, 2020.

Patel, P.K., Shirihai, O., and Huang, K.C., Optimal Dynamics for Quality Control in Spatially Distributed Mitochondrial Networks, Plos Computational Biology, vol. 9, pp. e1003108, 2013.

Pathak, D., Shields, L.Y., Mendelsohn, B.A., Haddad, D., Lin, W., Gerencser, A.A., Kim, H., Brand, M.D., Edwards, R.H., and Nakamura, K., The Role of Mitochondrially Derived ATP in Synaptic Vesicle Recycling, Journal of Biological Chemistry, vol. 290, pp. 22325-22336, 2015.

Pekkurnaz, G. and Wang, X., Mitochondrial heterogeneity and homeostasis through the lens of a neuron, Nature Metabolism, vol. 4, pp. 802-812, 2022.

Pissadaki, E.K. and Bolam, J.P., The energy cost of action potential propagation in dopamine neurons: clues to susceptibility in Parkinson's disease, Frontiers in Computational Neuroscience, vol. 7, pp. 13, 2013.

Puttrich, V., Rohlena, J., Braun, M., and Lansky, Z., In Vitro Reconstitution of Molecular Motor-Driven Mitochondrial Transport, Methods in Molecular Biology (Clifton, N.J.), vol. 2431, pp. 533-546, 2022.

Sheng, Z. and Cai, Q., Mitochondrial transport in neurons: impact on synaptic homeostasis and neurodegeneration, Nature Reviews Neuroscience, vol. 13, pp. 77-93, 2012.

Trushina, E., A shape shifting organelle: unusual mitochondrial phenotype determined with three-dimensional electron microscopy reconstruction, Neural Regeneration Research, vol. 11, pp. 900-901, 2016.

Vanhauwaert, R., Bharat, V., and Wang, X., Surveillance and transportation of mitochondria in neurons, Current Opinion in Neurobiology, vol. 57, pp. 87-93, 2019.

Xu, Z., Chu, X., Jiang, H., Schilling, H., Chen, S., and Feng, J., Induced dopaminergic neurons: A new promise for Parkinson's disease, Redox Biology, vol. 11, pp. 606-612, 2017.

Figure captions

Fig. 1. A schematic representation of a neuron with a symmetric branched axon (a) and an asymmetric branched axon (b). The diagram shows the compartment length closest to the proximal demand site. We assumed that all other compartments have equal lengths. The figure was created with the assistance of Servier Medical Art and is licensed under a Creative Commons Attribution 3.0 Generic License, available at http://smart.servier.com.

Fig. 2. A kinetic diagram representing a compartmental model of a branched axon. The compartments symbolize demand sites in the terminal, each represented by three compartments containing anterograde, stationary, and retrograde mitochondria. The diagram uses arrows to show the transport of mitochondria between transiting (anterograde and retrograde) states in neighboring demand sites. We assumed that mitochondria entering the terminal have a starting age of zero. Arrows in the diagram also depict the capture of mobile mitochondria into stationary states and their release from these states. Part (a) of the diagram displays a symmetrical branched axon, while part (b) displays an asymmetrical branched axon.

Fig. 3. The steady state values of the total length of stationary, anterogradely moving, and retrogradely moving mitochondria per unit length of the axon in the *i*-th demand site's compartment. (a) shows the results for a symmetric branched axon, and (b) displays the results for an asymmetric branched axon.

Fig. 4. Comparison of the average age of stationary, anterogradely moving, and retrogradely moving mitochondria in symmetric (a) and asymmetric (b) branched axons.

Fig. 5. Comparison of the age density distributions of anterogradely moving mitochondria in symmetric and asymmetric branched axons in various demand sites. (a) Demand sites 1, 4, 7. (b) Demand sites 8, 10, 14 (14 only for the symmetric axon).

Fig. 6. Comparison of the age density distributions of stationary mitochondria in symmetric and asymmetric branched axons in various demand sites. (a) Demand sites 1, 4, 7. (b) Demand sites 8, 10, 14 (14 only for the symmetric axon).

Fig. 7. Comparison of the age density distributions of retrograde moving mitochondria in symmetric and asymmetric branched axons in various demand sites. (a) Demand sites 1, 4, 7. (b) Demand sites 8, 10, 14 (14 only for the symmetric axon).

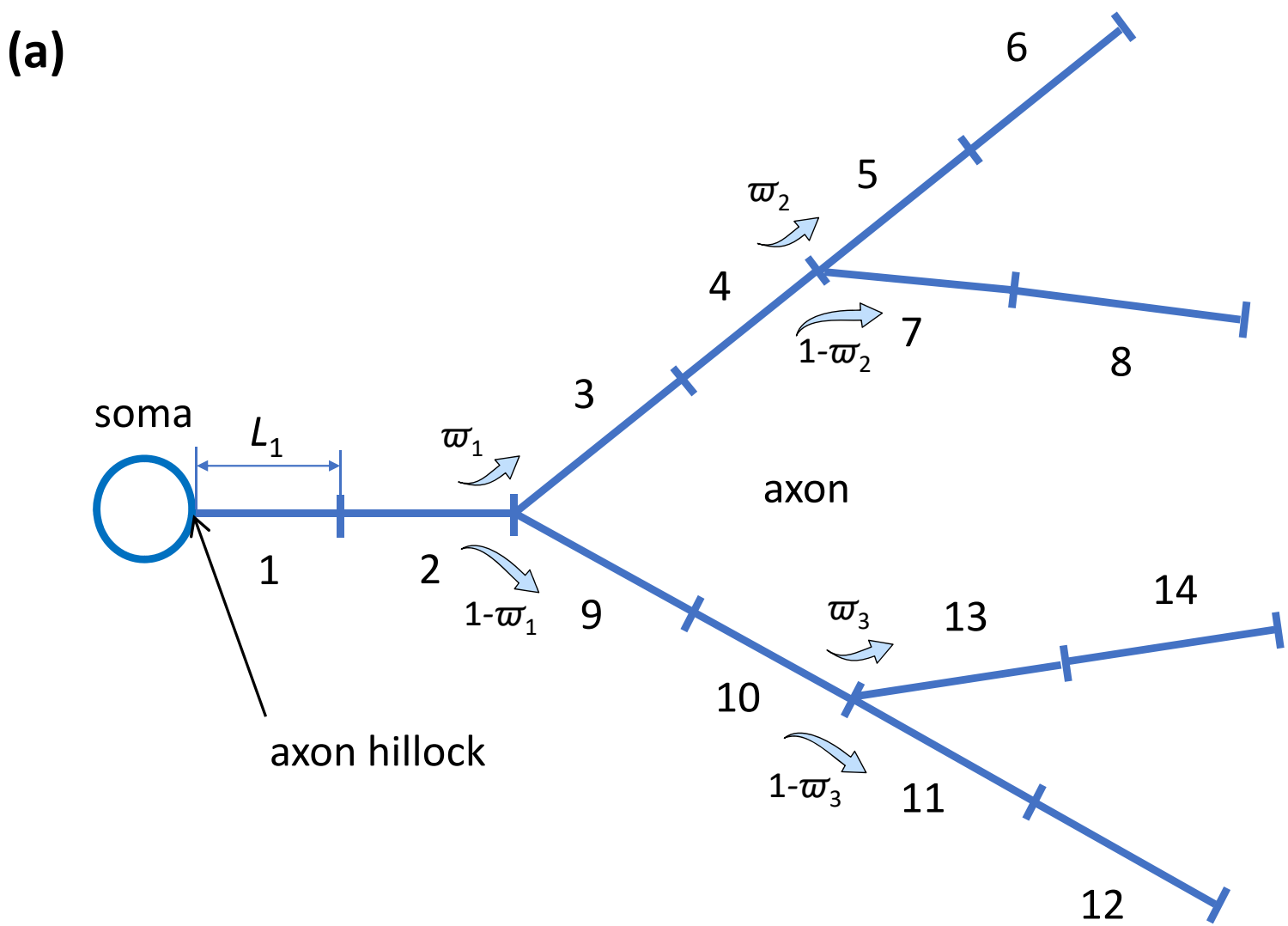
(a)
soma
L_1
axon hillock
1
2
3
4
5
6
7
8
9
10
11
12
13
14
ϖ_1
$1-\varpi_1$
ϖ_2
$1-\varpi_2$
ϖ_3
$1-\varpi_3$
axon

Figure 1a

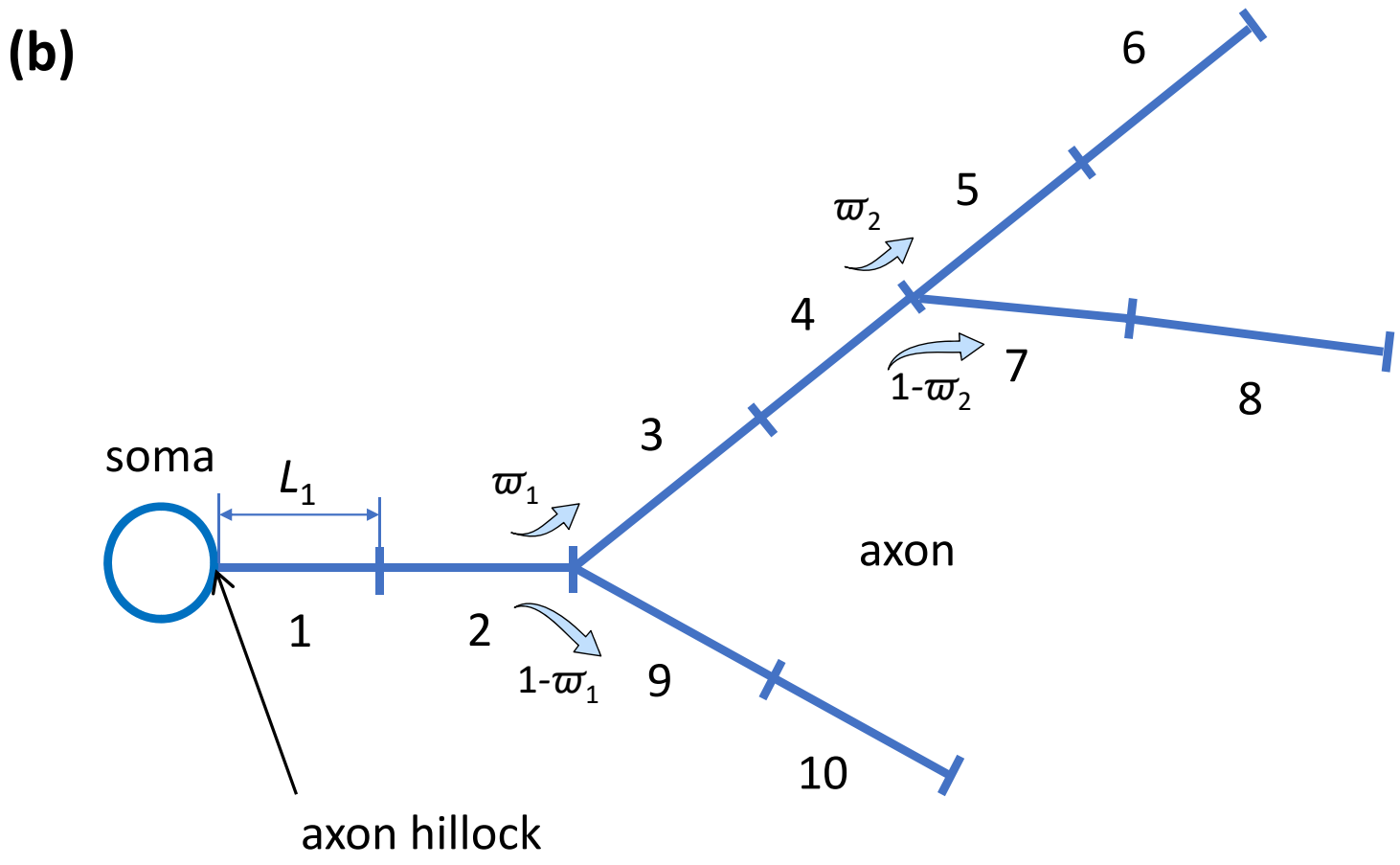
(b)
soma
L_1
ϖ_1
$1-\varpi_1$
ϖ_2
$1-\varpi_2$
axon
axon hillock
1
2
3
4
5
6
7
8
9
10

Figure 1b

(a)

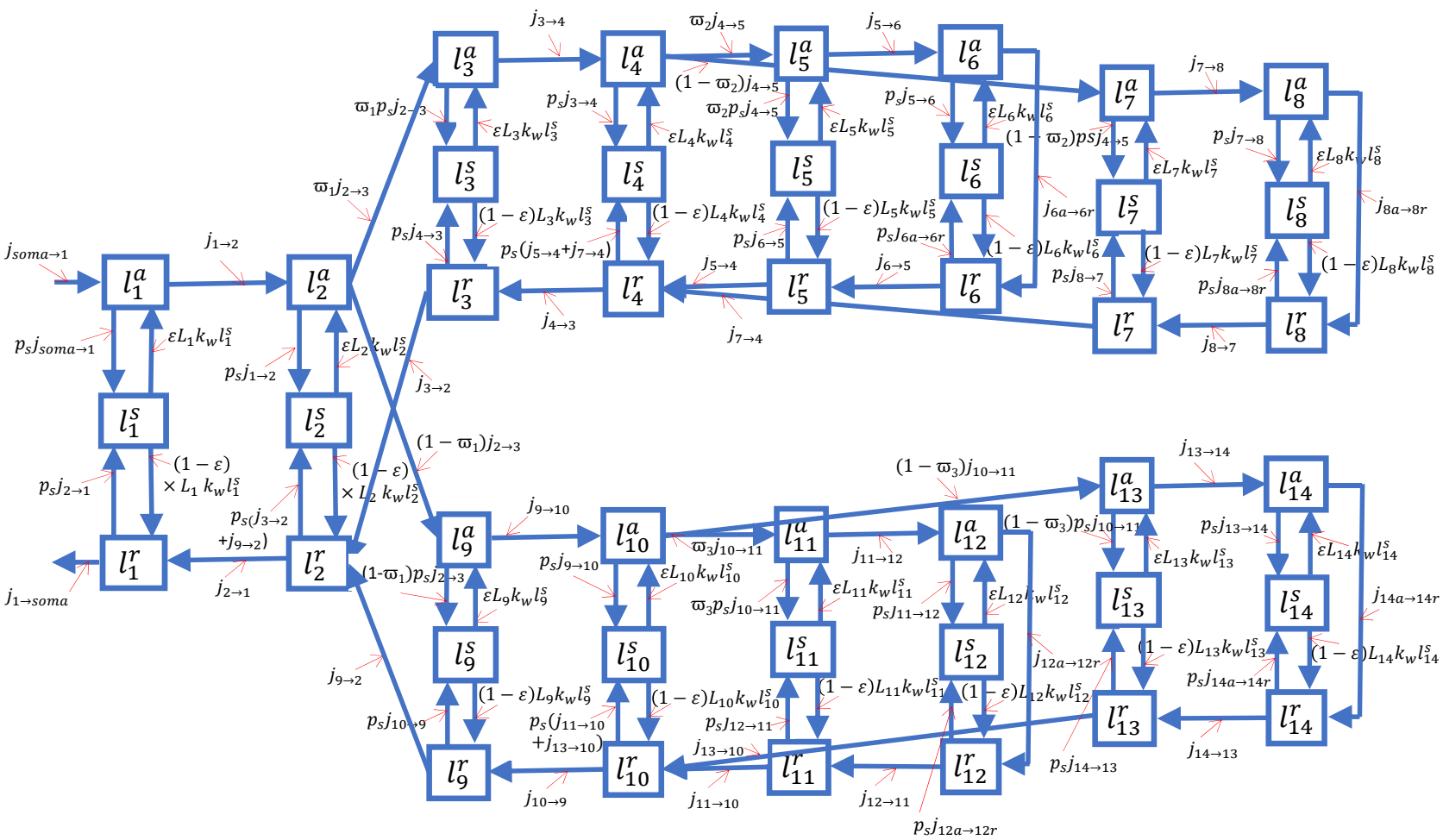
$j_{soma\to1}$
$j_{1\to2}$
$j_{1\to soma}$
$j_{2\to1}$
$j_{3\to4}$
$j_{4\to3}$
$j_{5\to6}$
$j_{6\to5}$
$j_{7\to8}$
$j_{8\to7}$
$j_{3\to2}$
$j_{9\to10}$
$j_{10\to9}$
$j_{11\to12}$
$j_{12\to11}$
$j_{13\to14}$
$j_{14\to13}$
$j_{5\to4}$
$j_{7\to4}$
$j_{9\to2}$
$j_{13\to10}$
$j_{11\to10}$
$j_{6a\to6r}$
$j_{8a\to8r}$
$j_{12a\to12r}$
$j_{14a\to14r}$
$\varepsilon L_1 k_w l_1^s$
$\varepsilon L_2 k_w l_2^s$
$\varepsilon L_3 k_w l_3^s$
$\varepsilon L_4 k_w l_4^s$
$\varepsilon L_5 k_w l_5^s$
$\varepsilon L_6 k_w l_6^s$
$\varepsilon L_7 k_w l_7^s$
$\varepsilon L_8 k_w l_8^s$
$\varepsilon L_9 k_w l_9^s$
$\varepsilon L_{10} k_w l_{10}^s$
$\varepsilon L_{11} k_w l_{11}^s$
$\varepsilon L_{12} k_w l_{12}^s$
$\varepsilon L_{13} k_w l_{13}^s$
$\varepsilon L_{14} k_w l_{14}^s$
$(1-\varepsilon) L_3 k_w l_3^s$
$(1-\varepsilon) L_4 k_w l_4^s$
$(1-\varepsilon) L_5 k_w l_5^s$
$(1-\varepsilon) L_6 k_w l_6^s$
$(1-\varepsilon) L_7 k_w l_7^s$
$(1-\varepsilon) L_8 k_w l_8^s$
$(1-\varepsilon) L_9 k_w l_9^s$
$(1-\varepsilon) L_{10} k_w l_{10}^s$
$(1-\varepsilon) L_{11} k_w l_{11}^s$
$(1-\varepsilon) L_{12} k_w l_{12}^s$
$(1-\varepsilon) L_{13} k_w l_{13}^s$
$(1-\varepsilon) L_{14} k_w l_{14}^s$
$(1-\varepsilon) \times L_1 k_w l_1^s$
$(1-\varepsilon) \times L_2 k_w l_2^s$
$p_s j_{soma\to1}$
$p_s j_{1\to2}$
$p_s j_{2\to1}$
$p_s j_{3\to2}$
$p_s j_{3\to4}$
$p_s j_{4\to3}$
$p_s j_{5\to6}$
$p_s j_{6\to5}$
$p_s j_{7\to8}$
$p_s j_{8\to7}$
$p_s j_{9\to10}$
$p_s j_{10\to9}$
$p_s j_{11\to12}$
$p_s j_{12\to11}$
$p_s j_{13\to14}$
$p_s j_{14\to13}$
$p_s j_{6a\to6r}$
$p_s j_{8a\to8r}$
$p_s j_{12a\to12r}$
$p_s j_{14a\to14r}$
$p_s j_{2\to3}$
$p_s j_{4\to5}$
$p_s j_{10\to11}$
$p_s j_{11\to10}$
$p_s j_{12\to13}$
$p_s j_{13\to12}$
$p_s (j_{3\to2} + j_{9\to2})$
$p_s (j_{5\to4} + j_{7\to4})$
$p_s (j_{11\to10} + j_{13\to10})$
$\varpi_1 j_{2\to3}$
$\varpi_1 p_s j_{2\to3}$
$(1-\varpi_1) j_{2\to3}$
$(1-\varpi_1) p_s j_{2\to3}$
$\varpi_2 j_{4\to5}$
$(1-\varpi_2) j_{4\to5}$
$\varpi_2 p_s j_{4\to5}$
$(1-\varpi_2) p_s j_{4\to5}$
$\varpi_3 j_{10\to11}$
$(1-\varpi_3) j_{10\to11}$
$\varpi_3 p_s j_{10\to11}$
$(1-\varpi_3) p_s j_{10\to11}$

Figure 2a

(b)

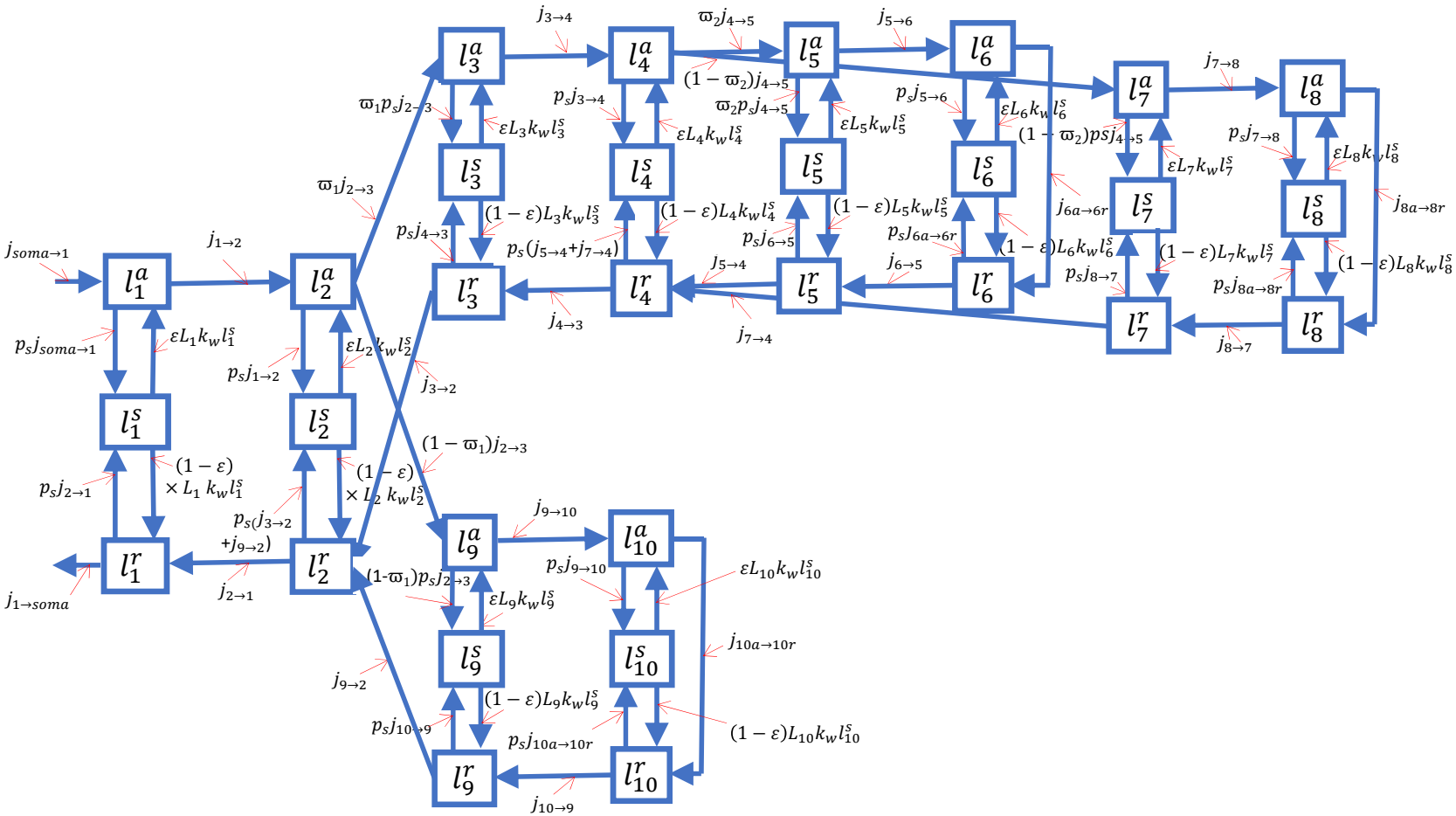
$j_{soma\to1}$
$j_{1\to2}$
$j_{3\to4}$
$\varpi_2 j_{4\to5}$
$j_{5\to6}$
$j_{7\to8}$
$\varpi_1 p_s j_{2\to3}$
$\varpi_1 j_{2\to3}$
$p_s j_{3\to4}$
$(1-\varpi_2)j_{4\to5}$
$\varpi_2 p_s j_{4\to5}$
$p_s j_{5\to6}$
$\varepsilon L_6 k_w l_6^s$
$(1-\varpi_2)ps j_{4\to5}$
$p_s j_{7\to8}$
$\varepsilon L_3 k_w l_3^s$
$\varepsilon L_4 k_w l_4^s$
$\varepsilon L_5 k_w l_5^s$
$\varepsilon L_7 k_w l_7^s$
$\varepsilon L_8 k_w l_8^s$
$(1-\varepsilon)L_3 k_w l_3^s$
$(1-\varepsilon)L_4 k_w l_4^s$
$(1-\varepsilon)L_5 k_w l_5^s$
$j_{6a\to6r}$
$j_{8a\to8r}$
$p_s j_{4\to3}$
$p_s(j_{5\to4}+j_{7\to4})$
$p_s j_{6\to5}$
$p_s j_{6a\to6r}$
$(1-\varepsilon)L_6 k_w l_6^s$
$(1-\varepsilon)L_7 k_w l_7^s$
$(1-\varepsilon)L_8 k_w l_8^s$
$j_{5\to4}$
$j_{6\to5}$
$p_s j_{8\to7}$
$p_s j_{8a\to8r}$
$j_{4\to3}$
$j_{7\to4}$
$j_{8\to7}$
$p_s j_{soma\to1}$
$\varepsilon L_1 k_w l_1^s$
$\varepsilon L_2 k_w l_2^s$
$p_s j_{1\to2}$
$j_{3\to2}$
$(1-\varpi_1)j_{2\to3}$
$p_s j_{2\to1}$
$(1-\varepsilon)$
$\times L_1\ k_w l_1^s$
$(1-\varepsilon)$
$\times L_2\ k_w l_2^s$
$p_s(j_{3\to2}$
$+j_{9\to2})$
$j_{9\to10}$
$(1-\varpi_1)p_s j_{2\to3}$
$p_s j_{9\to10}$
$\varepsilon L_{10} k_w l_{10}^s$
$j_{1\to soma}$
$j_{2\to1}$
$\varepsilon L_9 k_w l_9^s$
$j_{10a\to10r}$
$j_{9\to2}$
$(1-\varepsilon)L_9 k_w l_9^s$
$p_s j_{10\to9}$
$p_s j_{10a\to10r}$
$(1-\varepsilon)L_{10} k_w l_{10}^s$
$j_{10\to9}$

Figure 2b

(a)

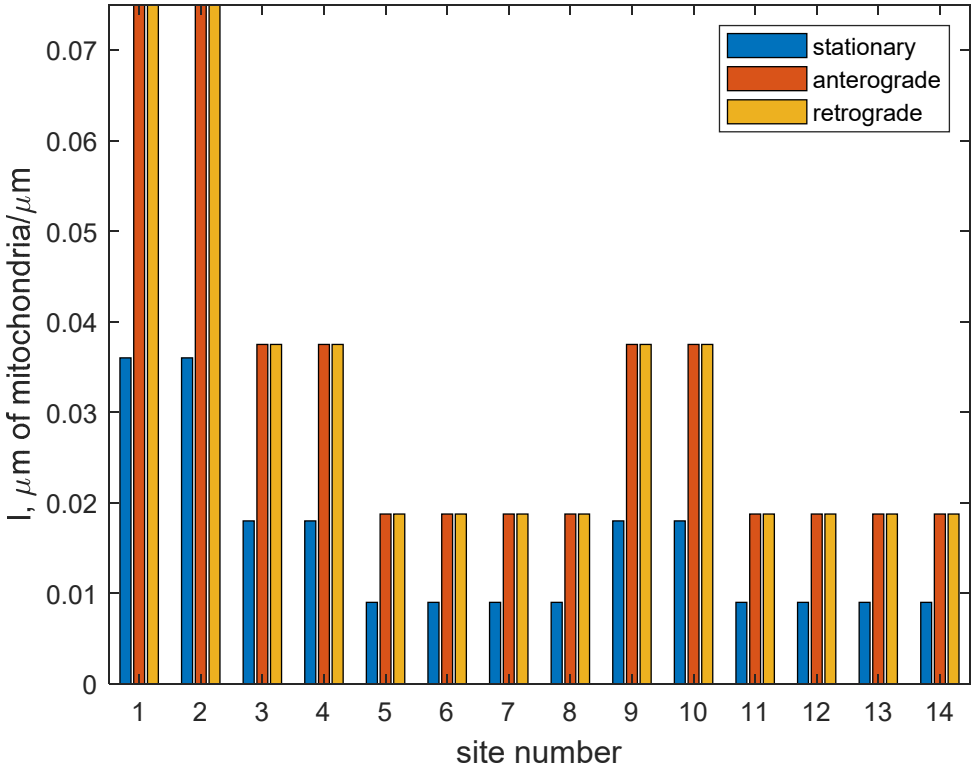

(b)

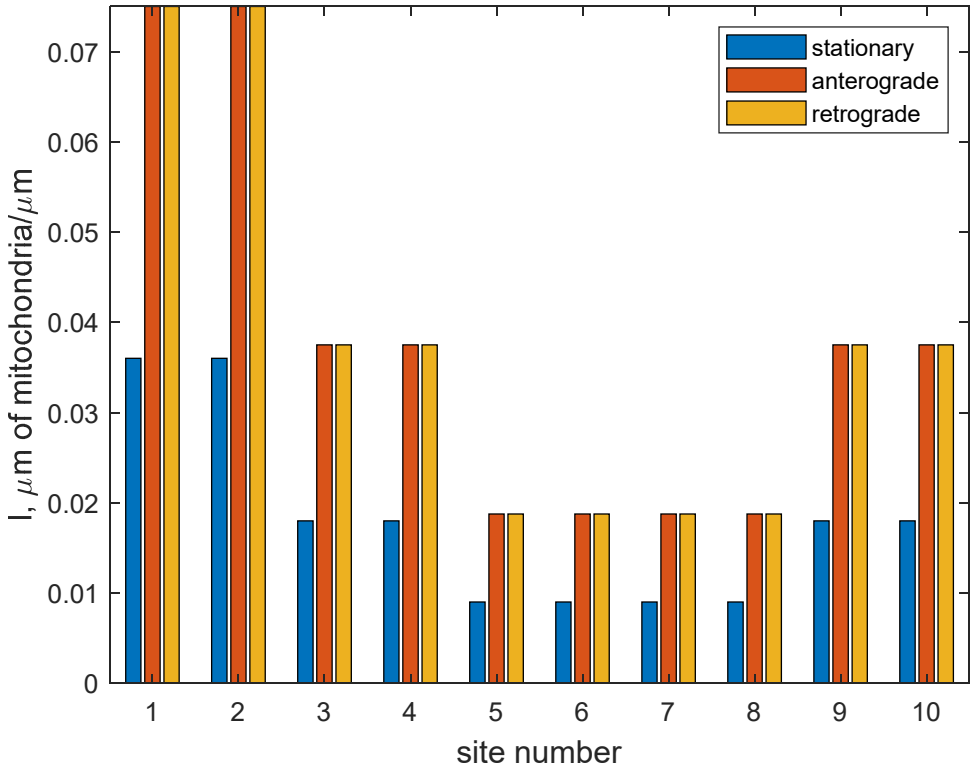

Figure 3a,b

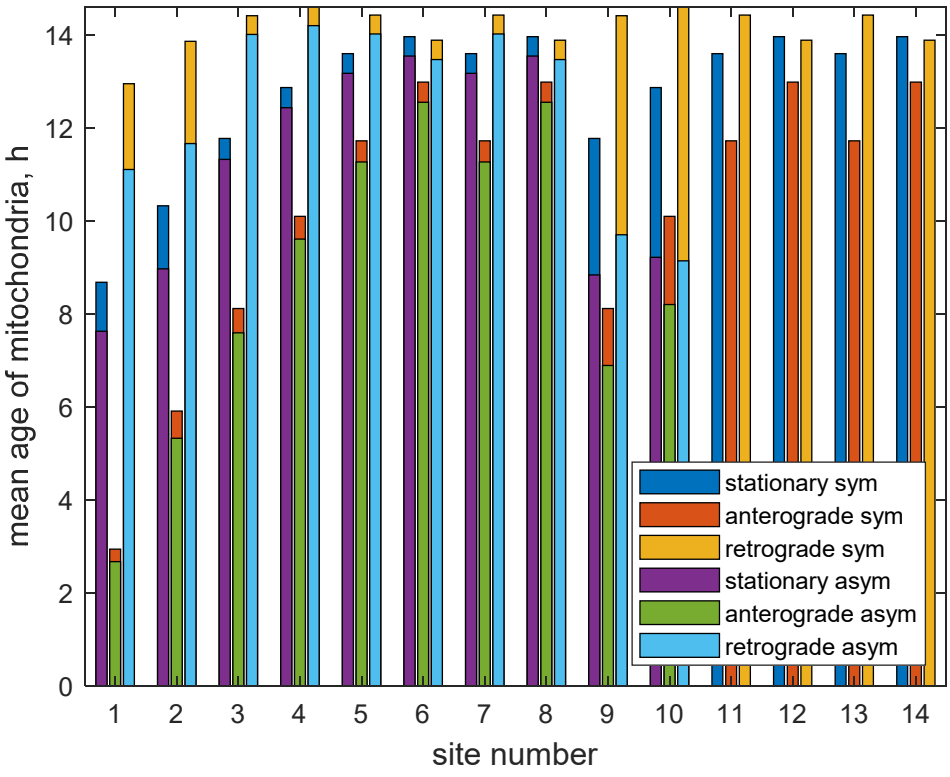
mean age of mitochondria, h
site number
0
2
4
6
8
10
12
14
1
2
3
4
5
6
7
8
9
10
11
12
13
14
stationary sym
anterograde sym
retrograde sym
stationary asym
anterograde asym
retrograde asym

Figure 4

(a)

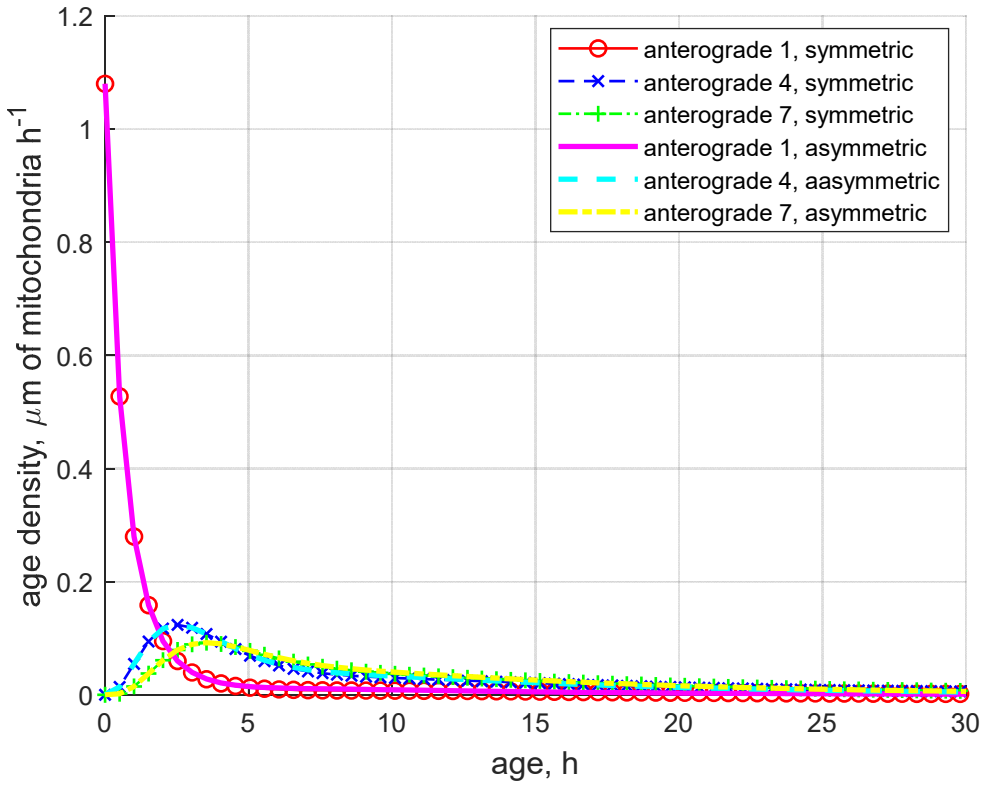

(b)

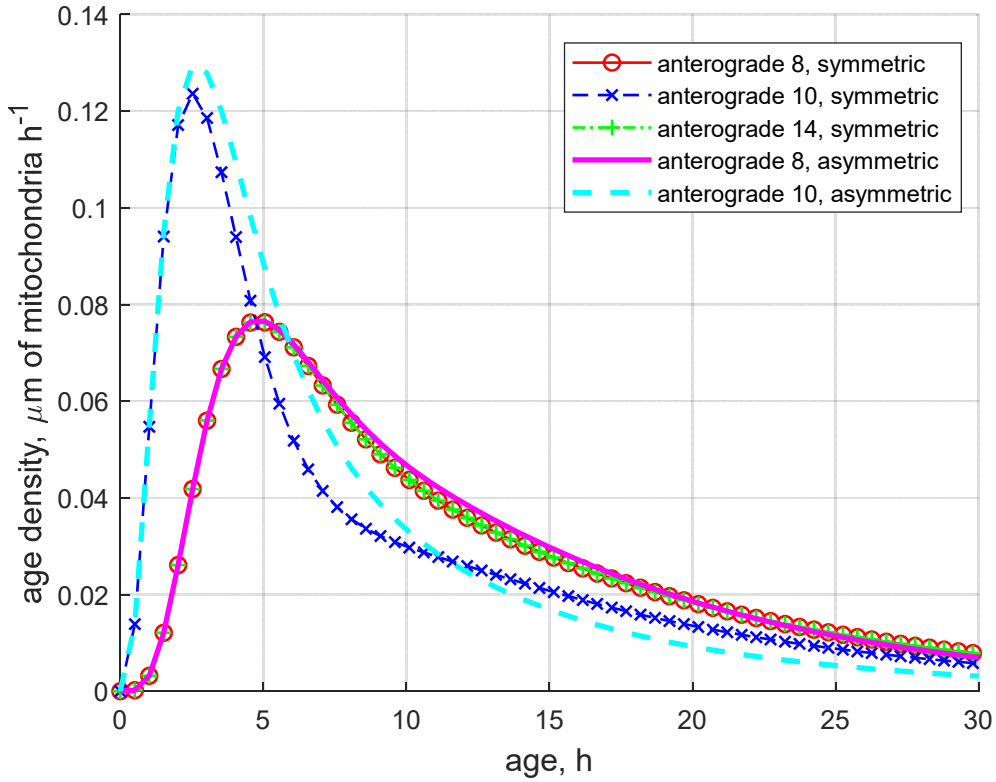

Figure 5a,b

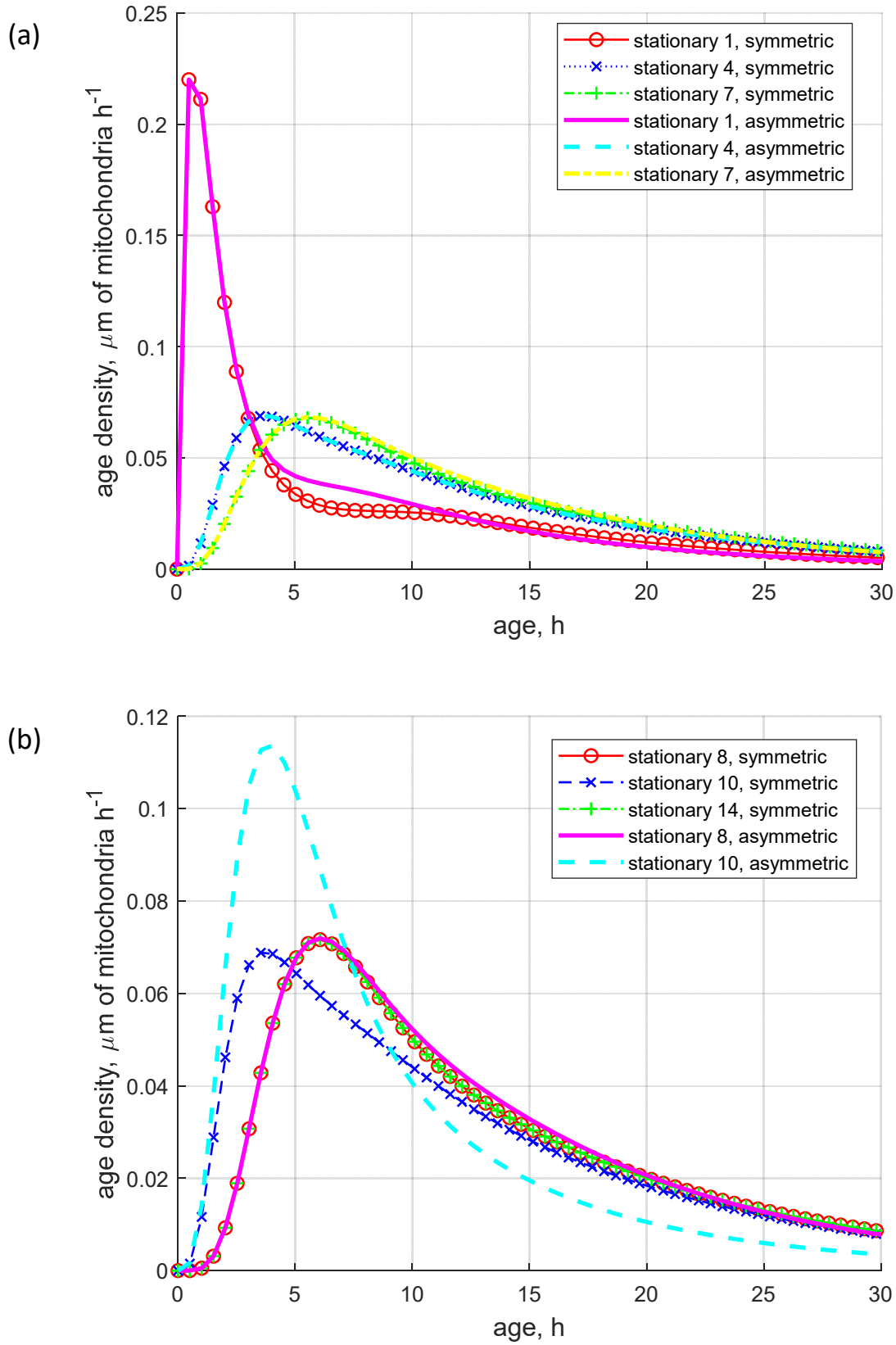
(a)
stationary 1, symmetric
stationary 4, symmetric
stationary 7, symmetric
stationary 1, asymmetric
stationary 4, asymmetric
stationary 7, asymmetric
age density, μm of mitochondria h-1
age, h
0.25
0.2
0.15
0.1
0.05
0
0
5
10
15
20
25
30
(b)
stationary 8, symmetric
stationary 10, symmetric
stationary 14, symmetric
stationary 8, asymmetric
stationary 10, asymmetric
age density, μm of mitochondria h-1
age, h
0.12
0.1
0.08
0.06
0.04
0.02
0
0
5
10
15
20
25
30

Figure 6a,b

(a)

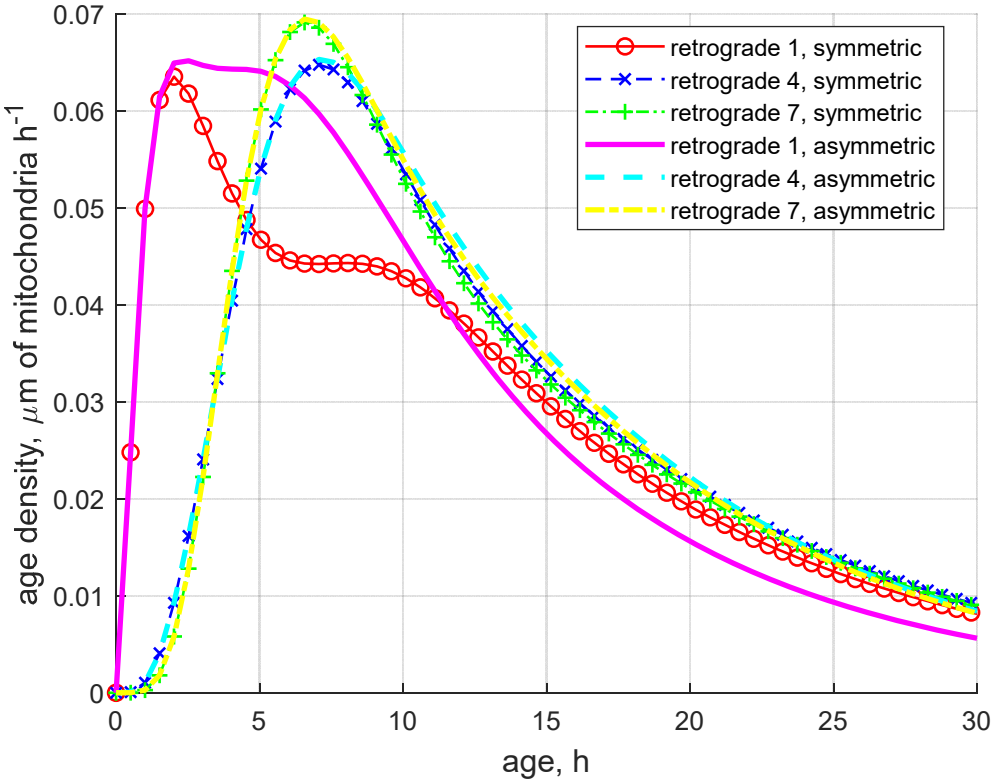

(b)

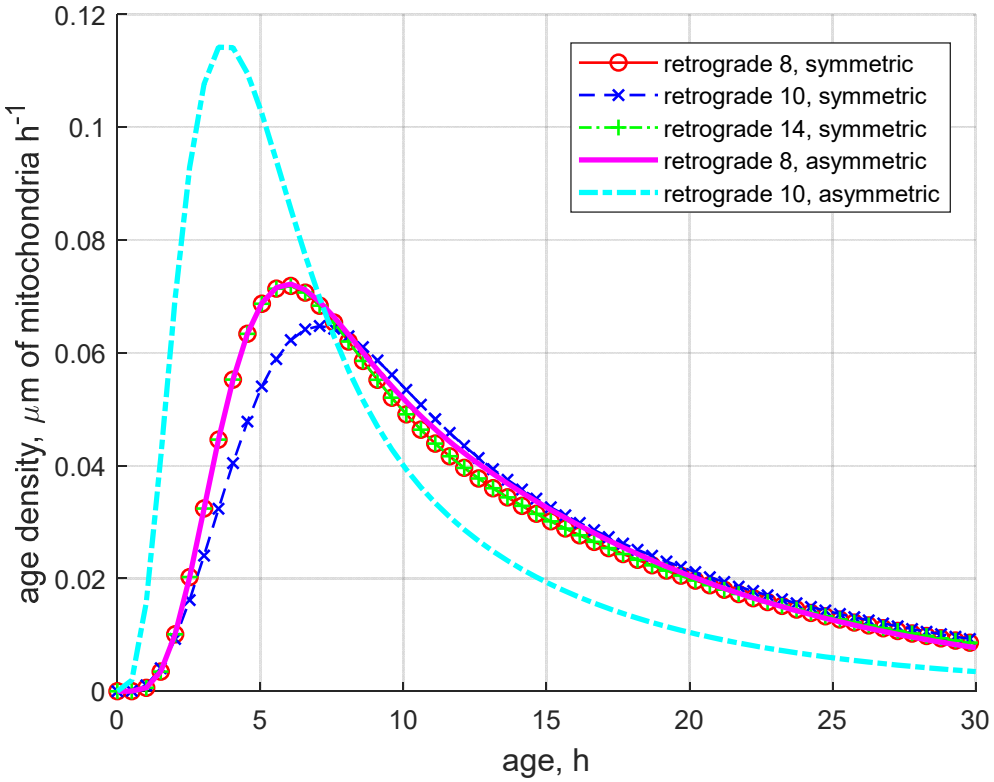

Figure 7a,b

Mitochondrial Transport in Axons with Multiple Branching Junctions: A Computational Study

Ivan A. Kuznetsov[(a), (b)] and Andrey V. Kuznetsov[(c)]

[(a)]Perelman School of Medicine, University of Pennsylvania, Philadelphia, PA 19104, USA

[(b)]Department of Bioengineering, University of Pennsylvania, Philadelphia, PA 19104, USA

[(c)]Dept. of Mechanical and Aerospace Engineering, North Carolina State University, Raleigh, NC 27695-7910, USA; e-mail: avkuznet@ncsu.edu

Supplemental Materials

S1. Governing equations for the case of an axon with two asymmetric branches (Figs. 1b and 2b)

S1.1. Equations that express the conservation of the total length of mitochondria in various compartments for an axon with two asymmetric branches (Figs. 1b and 2b)

Equations that are analogous to Eqs. (1)-(42) but now for the asymmetric axon displayed in Fig. 1b and 2b are

$$L_1 \frac{dl_1^s}{dt} = p_s \left(j_{soma\to 1} + j_{2\to 1} \right) - L_1 k_w l_1^s , \tag{S1}$$

$$L_1 \frac{dl_1^a}{dt} = j_{soma\to 1} - p_s j_{soma\to 1} - j_{1\to 2} + \varepsilon L_1 k_w l_1^s , \tag{S2}$$

$$L_1 \frac{dl_1^r}{dt} = j_{2\to 1} - p_s j_{2\to 1} - j_{1\to soma} + \left(1-\varepsilon\right) L_1 k_w l_1^s , \tag{S3}$$

$$L_2 \frac{dl_2^s}{dt} = p_s \left(j_{1\to 2} + j_{3\to 2} + j_{9\to 2} \right) - L_2 k_w l_2^s , \tag{S4}$$

$$L_2 \frac{dl_2^a}{dt} = j_{1\to 2} - p_s j_{1\to 2} - j_{2\to 3} + \varepsilon L_2 k_w l_2^s , \tag{S5}$$

$$L_2 \frac{dl_2^r}{dt} = j_{3\to 2} + j_{9\to 2} - p_s \left(j_{3\to 2} + j_{9\to 2} \right) - j_{2\to 1} + \left(1-\varepsilon\right) L_2 k_w l_2^s , \tag{S6}$$

$$L_3 \frac{dl_3^s}{dt} = p_s \left(\varpi_1 j_{2\to 3} + j_{4\to 3} \right) - L_3 k_w l_3^s , \tag{S7}$$

$$L_3 \frac{dl_3^a}{dt} = \varpi_1 j_{2\to3} - \varpi_1 p_s j_{2\to3} - j_{3\to4} + \varepsilon L_3 k_w l_3^s , \tag{S8}$$

$$L_3 \frac{dl_3^r}{dt} = j_{4\to3} - p_s j_{4\to3} - j_{3\to2} + \left(1-\varepsilon\right) L_3 k_w l_3^s , \tag{S9}$$

$$L_4 \frac{dl_4^s}{dt} = p_s \left(j_{3\to4} + j_{5\to4} + j_{7\to4} \right) - L_4 k_w l_4^s , \tag{S10}$$

$$L_4 \frac{dl_4^a}{dt} = j_{3\to4} - p_s j_{3\to4} - j_{4\to5} + \varepsilon L_4 k_w l_4^s , \tag{S11}$$

$$L_4 \frac{dl_4^r}{dt} = j_{5\to4} + j_{7\to4} - p_s \left(j_{5\to4} + j_{7\to4} \right) - j_{4\to3} + \left(1-\varepsilon\right) L_4 k_w l_4^s , \tag{S12}$$

$$L_5 \frac{dl_5^s}{dt} = p_s \left(\varpi_2 j_{4\to5} + j_{6\to5} \right) - L_5 k_w l_5^s , \tag{S13}$$

$$L_5 \frac{dl_5^a}{dt} = \varpi_2 j_{4\to5} - \varpi_2 p_s j_{4\to5} - j_{5\to6} + \varepsilon L_5 k_w l_5^s , \tag{S14}$$

$$L_5 \frac{dl_5^r}{dt} = j_{6\to5} - p_s j_{6\to5} - j_{5\to4} + \left(1-\varepsilon\right) L_5 k_w l_5^s , \tag{S15}$$

$$L_6 \frac{dl_6^s}{dt} = p_s \left(j_{5\to6} + j_{6a\to6r} \right) - L_6 k_w l_6^s , \tag{S16}$$

$$L_6 \frac{dl_6^a}{dt} = j_{5\to6} - p_s j_{5\to6} - j_{6a\to6r} + \varepsilon L_6 k_w l_6^s , \tag{S17}$$

$$L_6 \frac{dl_6^r}{dt} = j_{6a\to6r} - p_s j_{6a\to6r} - j_{6\to5} + \left(1-\varepsilon\right) L_6 k_w l_6^s , \tag{S18}$$

$$L_7 \frac{dl_7^s}{dt} = p_s \left(\left(1-\varpi_2\right) j_{4\to5} + j_{8\to7} \right) - L_7 k_w l_7^s , \tag{S19}$$

$$L_7 \frac{dl_7^a}{dt} = \left(1-\varpi_2\right) j_{4\to5} - p_s \left(1-\varpi_2\right) j_{4\to5} - j_{7\to8} + \varepsilon L_7 k_w l_7^s , \tag{S20}$$

$$L_7 \frac{dl_7^r}{dt} = j_{8\to7} - p_s j_{8\to7} - j_{7\to4} + \left(1-\varepsilon\right) L_7 k_w l_7^s , \tag{S21}$$

$$L_8 \frac{dl_8^s}{dt} = p_s \left(j_{7\to8} + j_{8a\to8r} \right) - L_8 k_w l_8^s , \tag{S22}$$

$$L_8 \frac{dl_8^a}{dt} = j_{7\to 8} - p_s j_{7\to 8} - j_{8a\to 8r} + \varepsilon L_8 k_w l_8^s , \tag{S23}$$

$$L_8 \frac{dl_8^r}{dt} = j_{8a\to 8r} - p_s j_{8a\to 8r} - j_{8\to 7} + \left(1-\varepsilon\right) L_8 k_w l_8^s , \tag{S24}$$

$$L_9 \frac{dl_9^s}{dt} = \left(1-\varpi_1\right) p_s j_{2\to 3} + p_s j_{10\to 9} - L_9 k_w l_9^s , \tag{S25}$$

$$L_9 \frac{dl_9^a}{dt} = \left(1-\varpi_1\right) j_{2\to 3} - p_s \left(1-\varpi_1\right) j_{2\to 3} - j_{9\to 10} + \varepsilon L_9 k_w l_9^s , \tag{S26}$$

$$L_9 \frac{dl_9^r}{dt} = j_{10\to 9} - p_s j_{10\to 9} - j_{9\to 2} + \left(1-\varepsilon\right) L_9 k_w l_9^s , \tag{S27}$$

$$L_{10} \frac{dl_{10}^s}{dt} = p_s j_{9\to 10} + p_s j_{10a\to 10r} - L_{10} k_w l_{10}^s , \tag{S28}$$

$$L_{10} \frac{dl_{10}^a}{dt} = j_{9\to 10} - p_s j_{9\to 10} - j_{10a\to 10r} + \varepsilon L_{10} k_w l_{10}^s , \tag{S29}$$

$$L_{10} \frac{dl_{10}^r}{dt} = j_{10a\to 10r} - p_s j_{10a\to 10r} - j_{10\to 9} + \left(1-\varepsilon\right) L_{10} k_w l_{10}^s . \tag{S30}$$

Equations that are analogous to Eqs. (43)-(70) but now for the asymmetric axon displayed in Fig. 1b are as follows. Equations for anterograde fluxes (Fig. 2b) now are

$$j_{1\to 2} = v_a l_1^a , \tag{S31}$$

$$j_{2\to 3} = v_a l_2^a , \tag{S32}$$

$$j_{3\to 4} = v_a l_3^a , \tag{S33}$$

$$j_{4\to 5} = v_a l_4^a , \tag{S34}$$

$$j_{5\to 6} = v_a l_5^a , \tag{S35}$$

$$j_{7\to 8} = v_a l_7^a , \tag{S36}$$

$$j_{9\to 10} = v_a l_9^a . \tag{S37}$$

Equations for retrograde fluxes (Fig. 2b) now are

$$j_{1\to soma} = v_r l_1^r , \tag{S38}$$

$$j_{2\to 1} = v_r l_2^r \,, \tag{S39}$$

$$j_{3\to 2} = v_r l_3^r \,, \tag{S40}$$

$$j_{4\to 3} = v_r l_4^r \,, \tag{S41}$$

$$j_{5\to 4} = v_r l_5^r \,, \tag{S42}$$

$$j_{6\to 5} = v_r l_6^r \,, \tag{S43}$$

$$j_{7\to 4} = v_r l_7^r \,, \tag{S44}$$

$$j_{8\to 7} = v_r l_8^r \,, \tag{S45}$$

$$j_{9\to 2} = v_r l_9^r \,, \tag{S46}$$

$$j_{10\to 9} = v_r l_{10}^r \,. \tag{S47}$$

The turn-around fluxes (Fig. 2b) now are simulated as follows:

$$j_{6a\to 6r} = v_a l_6^a \,, \tag{S48}$$

$$j_{8a\to 8r} = v_a l_8^a \,, \tag{S49}$$

$$j_{10a\to 10r} = v_a l_{10}^a \,. \tag{S50}$$

S1.2. Model of mean age and age density distributions of mitochondria in the demand sites for the asymmetric axon displayed in Figs. 1b and 2b

Equations that are analogous to Eqs. (74)-(201) but now for the asymmetric axon displayed in Figs. 1b and 2b are

$$b_{1,1} = -L_1 k_w l_1^s \,/\left(L_1 l_1^s\right), \tag{S51}$$

$$b_{N+1,N+1} = -\left(p_s j_{soma\to 1} + j_{1\to 2}\right)/\left(L_1 l_1^a\right), \tag{S52}$$

$$b_{2N+1,2N+1} = -\left(p_s j_{2\to 1} + j_{1\to soma}\right)/\left(L_1 l_1^r\right), \tag{S53}$$

$$b_{N+1,1} = \varepsilon L_1 k_w l_1^s \,/\left(L_1 l_1^s\right), \tag{S54}$$

$$b_{1,N+1} = p_s j_{soma\to 1} / \left(L_1 l_1^a \right), \tag{S55}$$

$$b_{2N+1,1} = \left(1-\varepsilon\right) L_1 k_w l_1^s / \left(L_1 l_1^s \right), \tag{S56}$$

$$b_{1,2N+1} = p_s j_{2\to 1} / \left(L_1 l_1^r \right), \tag{S57}$$

$$b_{N+2,N+1} = j_{1\to 2} / \left(L_1 l_1^a \right), \tag{S58}$$

$$b_{2N+1,2N+2} = j_{2\to 1} / \left(L_2 l_2^r \right), \tag{S59}$$

$$b_{2,2} = -L_2 k_w l_2^s / \left(L_2 l_2^s \right), \tag{S60}$$

$$b_{N+2,N+2} = -\left(p_s j_{1\to 2} + j_{2\to 3} \right) / \left(L_2 l_2^a \right), \tag{S61}$$

$$b_{2N+2,2N+2} = -\left(p_s j_{3\to 2} + p_s j_{9\to 2} + j_{2\to 1} \right) / \left(L_2 l_2^r \right), \tag{S62}$$

$$b_{N+2,2} = \varepsilon L_2 k_w l_2^s / \left(L_2 l_2^s \right), \tag{S63}$$

$$b_{2,N+2} = p_s j_{1\to 2} / \left(L_2 l_2^a \right), \tag{S64}$$

$$b_{2N+2,2} = \left(1-\varepsilon\right) L_2 k_w l_2^s / \left(L_2 l_2^s \right), \tag{S65}$$

$$b_{2,2N+2} = p_s \left(j_{3\to 2} + j_{9\to 2} \right) / \left(L_2 l_2^r \right), \tag{S66}$$

$$b_{N+9,N+2} = \left(1-\varpi_1\right) j_{2\to 3} / \left(L_2 l_2^a \right), \tag{S67}$$

$$b_{N+3,N+2} = \varpi_1 j_{2\to 3} / \left(L_2 l_2^a \right), \tag{S68}$$

$$b_{3,3} = -L_3 k_w l_3^s / \left(L_3 l_3^s \right), \tag{S69}$$

$$b_{N+3,N+3} = -\left(\varpi_1 p_s j_{2\to 3} + j_{3\to 4} \right) / \left(L_3 l_3^a \right), \tag{S70}$$

$$b_{2N+3,2N+3} = -\left(p_s j_{4\to 3} + j_{3\to 2} \right) / \left(L_3 l_3^r \right), \tag{S71}$$

$$b_{N+3,3} = \varepsilon L_3 k_w l_3^s / \left(L_3 l_3^s \right), \tag{S72}$$

$$b_{3,N+3} = \varpi_1 p_s j_{2\to 3} / \left(L_3 l_3^a \right), \tag{S73}$$

$$b_{2N+3,3} = (1-\varepsilon) L_3 k_w l_3^s / \left(L_3 l_3^s\right), \tag{S74}$$

$$b_{3,2N+3} = p_s j_{4\to 3} / \left(L_3 l_3^r\right), \tag{S75}$$

$$b_{N+4,N+3} = j_{3\to 4} / \left(L_3 l_3^a\right), \tag{S76}$$

$$b_{4,N+4} = p_s j_{3\to 4} / \left(L_4 l_4^a\right), \tag{S77}$$

$$b_{4,4} = -L_4 k_w l_4^s / \left(L_4 l_4^s\right), \tag{S78}$$

$$b_{N+4,N+4} = -\left(p_s j_{3\to 4} + j_{4\to 5}\right) / \left(L_4 l_4^a\right), \tag{S79}$$

$$b_{N+5,N+4} = \varpi_2 j_{4\to 5} / \left(L_4 l_4^a\right), \tag{S80}$$

$$b_{N+7,N+4} = (1-\varpi_2) j_{4\to 5} / \left(L_4 l_4^a\right), \tag{S81}$$

$$b_{2N+4,2N+4} = -\left(p_s j_{5\to 4} + p_s j_{7\to 4} + j_{4\to 3}\right) / \left(L_4 l_4^r\right), \tag{S82}$$

$$b_{N+4,4} = \varepsilon L_4 k_w l_4^s / \left(L_4 l_4^s\right), \tag{S83}$$

$$b_{2N+4,4} = (1-\varepsilon) L_4 k_w l_4^s / \left(L_4 l_4^s\right), \tag{S84}$$

$$b_{4,2N+4} = p_s \left(j_{5\to 4} + j_{7\to 4}\right) / \left(L_4 l_4^r\right), \tag{S85}$$

$$b_{2N+3,2N+4} = j_{4\to 3} / \left(L_4 l_4^r\right), \tag{S86}$$

$$b_{2N+2,2N+3} = j_{3\to 2} / \left(L_3 l_3^r\right), \tag{S87}$$

$$b_{N+6,N+5} = j_{5\to 6} / \left(L_5 l_5^a\right), \tag{S88}$$

$$b_{5,5} = -L_5 k_w l_5^s / \left(L_5 l_5^s\right), \tag{S89}$$

$$b_{N+5,N+5} = -\left(\varpi_2 p_s j_{4\to 5} + j_{5\to 6}\right) / \left(L_5 l_5^a\right), \tag{S90}$$

$$b_{2N+5,2N+5} = -\left(p_s j_{6\to 5} + j_{5\to 4}\right) / \left(L_5 l_5^r\right), \tag{S91}$$

$$b_{2N+4,2N+5} = j_{5\to 4} / \left(L_5 l_5^r\right), \tag{S92}$$

$$b_{N+5,5} = \varepsilon L_5 k_w l_5^s / \left(L_5 l_5^s \right), \tag{S93}$$

$$b_{5,N+5} = \varpi_2 p_s j_{4\to5} / \left(L_5 l_5^a \right), \tag{S94}$$

$$b_{2N+5,5} = \left(1-\varepsilon\right) L_5 k_w l_5^s / \left(L_5 l_5^s \right), \tag{S95}$$

$$b_{5,2N+5} = p_s j_{6\to5} / \left(L_5 l_5^r \right), \tag{S96}$$

$$b_{6,N+6} = p_s j_{5\to6} / \left(L_6 l_6^a \right), \tag{S97}$$

$$b_{6,6} = -L_6 k_w l_6^s / \left(L_6 l_6^s \right), \tag{S98}$$

$$b_{N+6,N+6} = -\left(p_s j_{5\to6} + j_{6a\to6r} \right) / \left(L_6 l_6^a \right), \tag{S99}$$

$$b_{2N+6,2N+6} = -\left(p_s j_{6a\to6r} + j_{6\to5} \right) / \left(L_6 l_6^r \right), \tag{S100}$$

$$b_{N+6,6} = \varepsilon L_6 k_w l_6^s / \left(L_6 l_6^s \right), \tag{S101}$$

$$b_{6,2N+6} = p_s j_{6a\to6r} / \left(L_6 l_6^r \right), \tag{S102}$$

$$b_{2N+6,6} = \left(1-\varepsilon\right) L_6 k_w l_6^s / \left(L_6 l_6^s \right), \tag{S103}$$

$$b_{2N+5,2N+6} = j_{6\to5} / \left(L_6 l_6^r \right), \tag{S104}$$

$$b_{2N+6,N+6} = j_{6a\to6r} / \left(L_6 l_6^a \right), \tag{S105}$$

$$b_{7,N+7} = \left(1-\varpi_2\right) p_s j_{4\to5} / \left(L_7 l_7^a \right), \tag{S106}$$

$$b_{7,7} = -L_7 k_w l_7^s / \left(L_7 l_7^s \right), \tag{S107}$$

$$b_{N+7,N+7} = -\left(\left(1-\varpi_2\right) p_s j_{4\to5} + j_{7\to8} \right) / \left(L_7 l_7^a \right), \tag{S108}$$

$$b_{N+8,N+7} = j_{7\to8} / \left(L_7 l_7^a \right), \tag{S109}$$

$$b_{2N+7,2N+7} = -\left(p_s j_{8\to7} + j_{7\to4} \right) / \left(L_7 l_7^r \right), \tag{S110}$$

$$b_{7,2N+7} = p_s j_{8\to7} / \left(L_7 l_7^r \right), \tag{S111}$$

$$b_{N+7,7} = \varepsilon L_7 k_w l_7^s / \left(L_7 l_7^s \right), \tag{S112}$$

$$b_{2N+7,7} = \left(1-\varepsilon\right) L_7 k_w l_7^s / \left(L_7 l_7^s \right), \tag{S113}$$

$$b_{2N+4,2N+7} = j_{7\to 4} / \left(L_7 l_7^r \right), \tag{S114}$$

$$b_{8,N+8} = p_s j_{7\to 8} / \left(L_8 l_8^a \right), \tag{S115}$$

$$b_{8,8} = -L_8 k_w l_8^s / \left(L_8 l_8^s \right), \tag{S116}$$

$$b_{N+8,N+8} = -\left(p_s j_{7\to 8} + j_{8a\to 8r} \right) / \left(L_8 l_8^a \right), \tag{S117}$$

$$b_{2N+8,2N+8} = -\left(p_s j_{8a\to 8r} + j_{8\to 7} \right) / \left(L_8 l_8^r \right), \tag{S118}$$

$$b_{8,2N+8} = p_s j_{8a\to 8r} / \left(L_8 l_8^r \right), \tag{S119}$$

$$b_{2N+7,2N+8} = j_{8\to 7} / \left(L_8 l_8^r \right), \tag{S120}$$

$$b_{N+8,8} = \varepsilon L_8 k_w l_8^s / \left(L_8 l_8^s \right), \tag{S121}$$

$$b_{2N+8,8} = \left(1-\varepsilon\right) L_8 k_w l_8^s / \left(L_8 l_8^s \right), \tag{S122}$$

$$b_{2N+8,N+8} = j_{8a\to 8r} / \left(L_8 l_8^a \right), \tag{S123}$$

$$b_{9,N+9} = \left(1-\varpi_1\right) p_s j_{2\to 3} / \left(L_9 l_9^a \right), \tag{S124}$$

$$b_{9,9} = -L_9 k_w l_9^s / \left(L_9 l_9^s \right), \tag{S125}$$

$$b_{N+9,N+9} = -\left(\left(1-\varpi_1\right) p_s j_{2\to 3} + j_{9\to 10} \right) / \left(L_9 l_9^a \right), \tag{S126}$$

$$b_{2N+9,2N+9} = -\left(p_s j_{10\to 9} + j_{9\to 2} \right) / \left(L_9 l_9^r \right), \tag{S127}$$

$$b_{2N+2,2N+9} = j_{9\to 2} / \left(L_9 l_9^r \right), \tag{S128}$$

$$b_{N+9,9} = \varepsilon L_9 k_w l_9^s / \left(L_9 l_9^s \right), \tag{S129}$$

$$b_{2N+9,9} = \left(1-\varepsilon\right) L_9 k_w l_9^s / \left(L_9 l_9^s \right), \tag{S130}$$

$$b_{9,2N+9} = p_s j_{10\to 9} / \left(L_9 l_9^r \right), \tag{S131}$$

$$b_{N+10,N+9} = j_{9\to 10} / \left(L_9 l_9^a \right), \tag{S132}$$

$$b_{10,N+10} = p_s j_{9\to 10} / \left(L_{10} l_{10}^a \right), \tag{S133}$$

$$b_{10,10} = -L_{10} k_w l_{10}^s / \left(L_{10} l_{10}^s \right), \tag{S134}$$

$$b_{N+10,N+10} = -\left(p_s j_{9\to 10} + j_{10a\to 10r} \right) / \left(L_{10} l_{10}^a \right), \tag{S135}$$

$$b_{2N+10,2N+10} = -\left(p_s j_{10a\to 10r} + j_{10\to 9} \right) / \left(L_{10} l_{10}^r \right), \tag{S136}$$

$$b_{2N+9,2N+10} = j_{10\to 9} / \left(L_{10} l_{10}^r \right), \tag{S137}$$

$$b_{N+10,10} = \varepsilon L_{10} k_w l_{10}^s / \left(L_{10} l_{10}^s \right), \tag{S138}$$

$$b_{2N+10,10} = \left(1-\varepsilon\right) L_{10} k_w l_{10}^s / \left(L_{10} l_{10}^s \right), \tag{S139}$$

$$b_{10,2N+10} = p_s j_{10a\to 10r} / \left(L_{10} l_{10}^r \right), \tag{S140}$$

$$b_{2N+10,N+10} = j_{10a\to 10r} / \left(L_{10} l_{10}^a \right), \tag{S141}$$

All other matrix B elements, except for those specified in Eqs. (S51)-(S141), are set to zero.

The only flux of mitochondria entering the axon is the anterograde flux from the soma to the compartment with anterograde mitochondria by the most proximal demand site, $j_{soma\to 1}$.

Our model assumes that all mitochondria that leave the axon (their flux is $j_{1\to soma}$) return to the soma for degradation, and none reenter the axon. The mitochondrial age in our model is thus understood as the amount of time that has passed since the mitochondria entered the axon.

The $(N+1)^{\text{th}}$ element of vector **u** is obtained from the following equation:

$$u_{N+1} = j_{soma\to 1}. \tag{S142}$$

As no other external fluxes enter the terminal,

$$u_i = 0 \quad (i=1,\ldots,N,N+2,\ldots,N+6,2N+1,\ldots,2N+10). \tag{S143}$$

S2. Supplementary figures

S2.1. Symmetric branched axon displayed in Figs. 1a and 2a

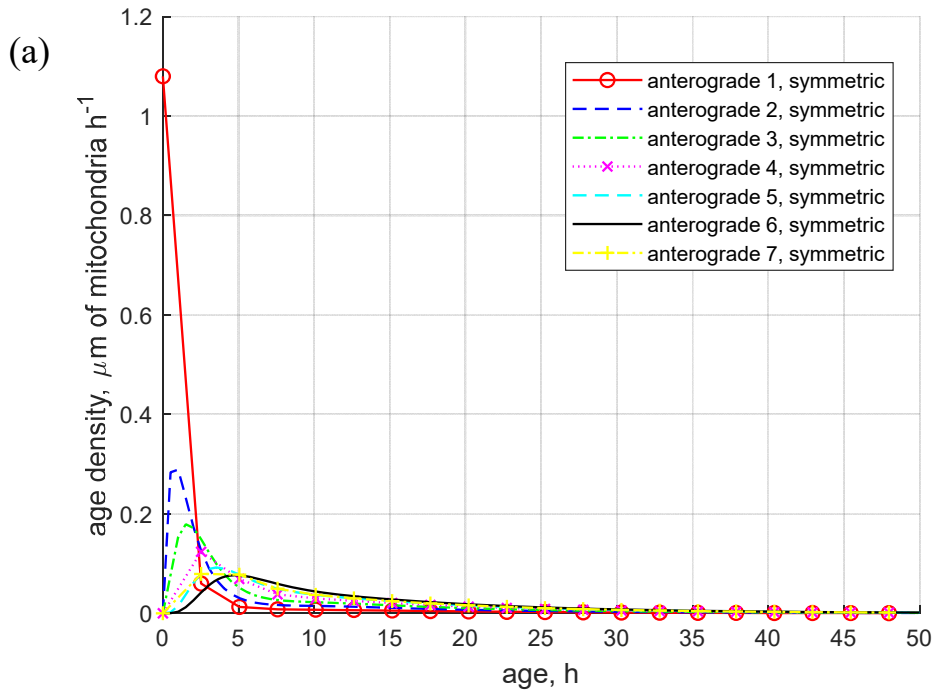

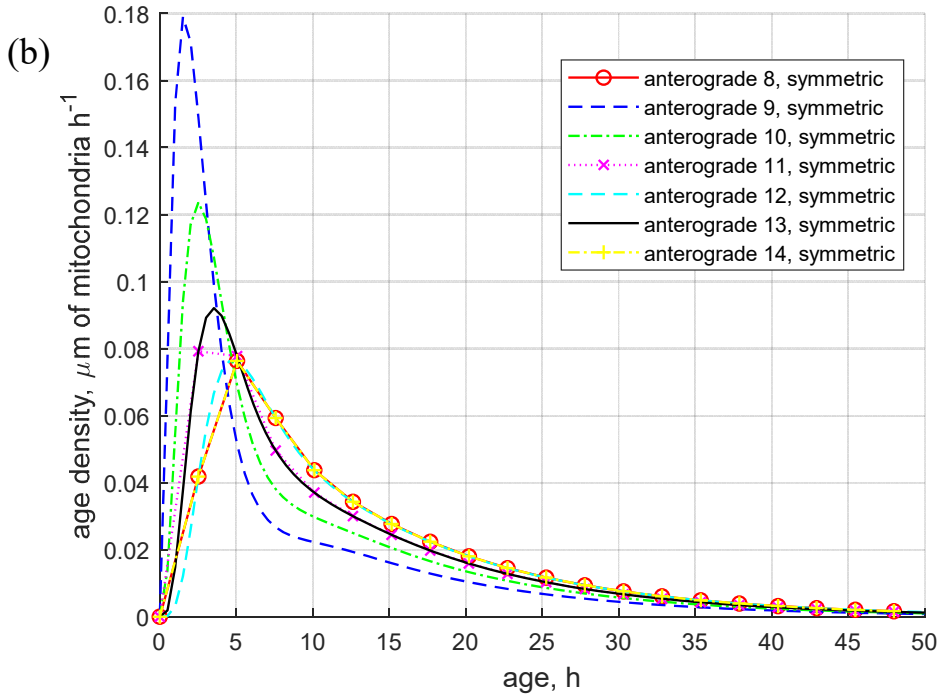

Fig. S1. Age density distributions of anterogradely moving mitochondria in a symmetric branched axon across various demand sites. (a) Demand sites 1 to 7; (b) Demand sites 8 to 14.

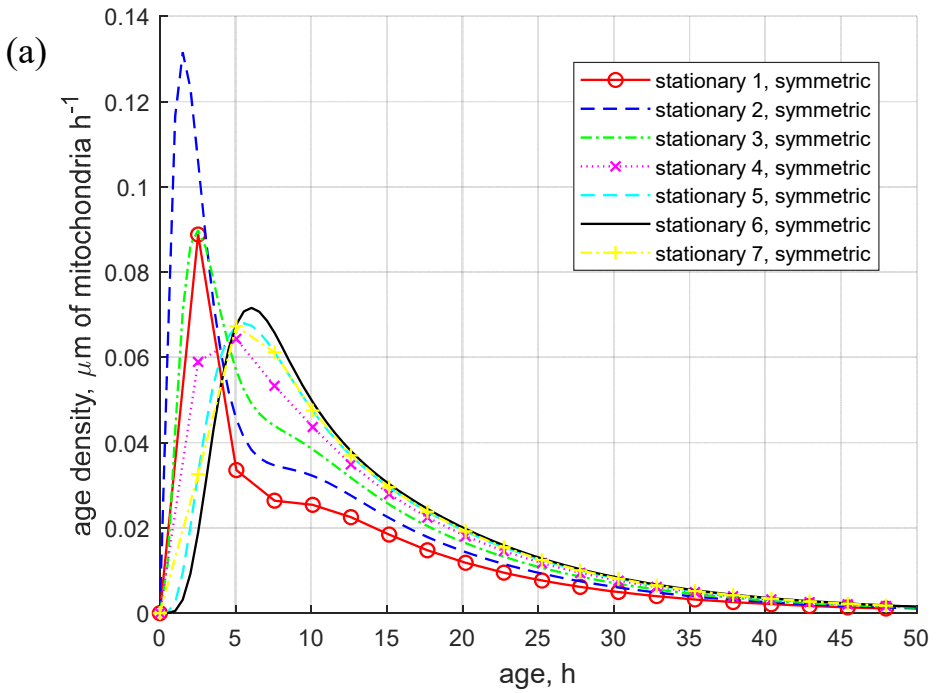

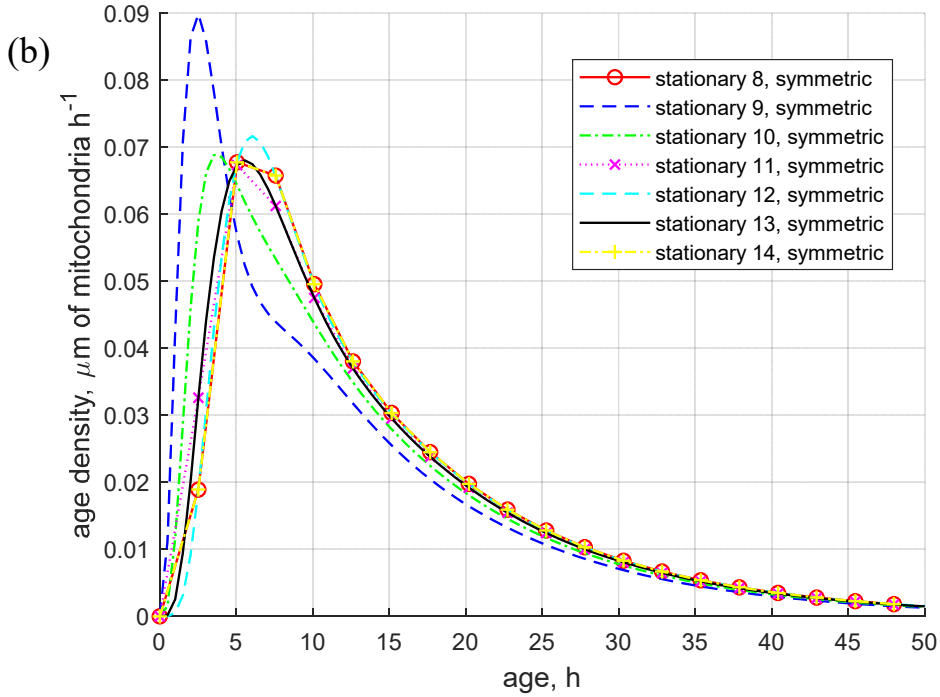

Fig. S2. Age density distributions of stationary mitochondria in a symmetric branched axon across various demand sites. (a) Demand sites 1 to 7; (b) Demand sites 8 to 14.

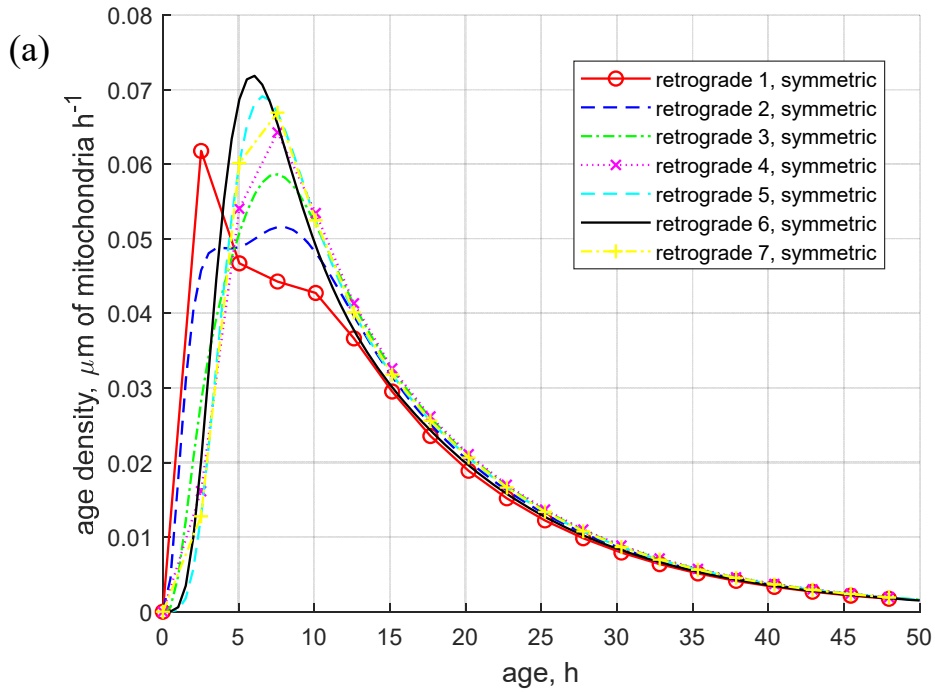

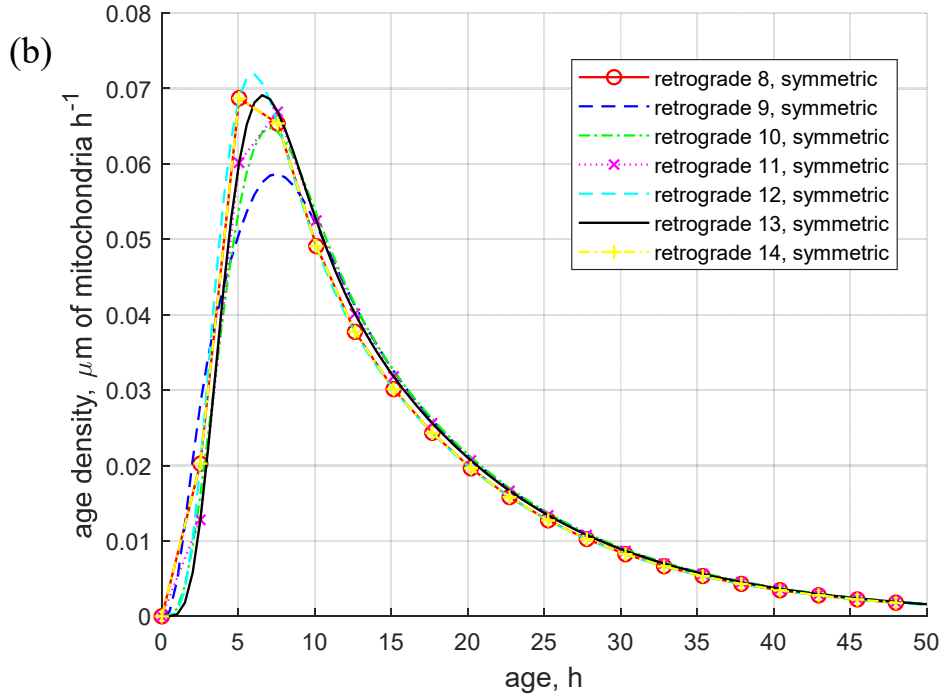

Fig. S3. Age density distributions of retrogradely moving mitochondria in a symmetric branched axon across various demand sites. (a) Demand sites 1 to 7; (b) Demand sites 8 to 14.

S2.2. Asymmetric branched axon displayed in Figs. 1b and 2b

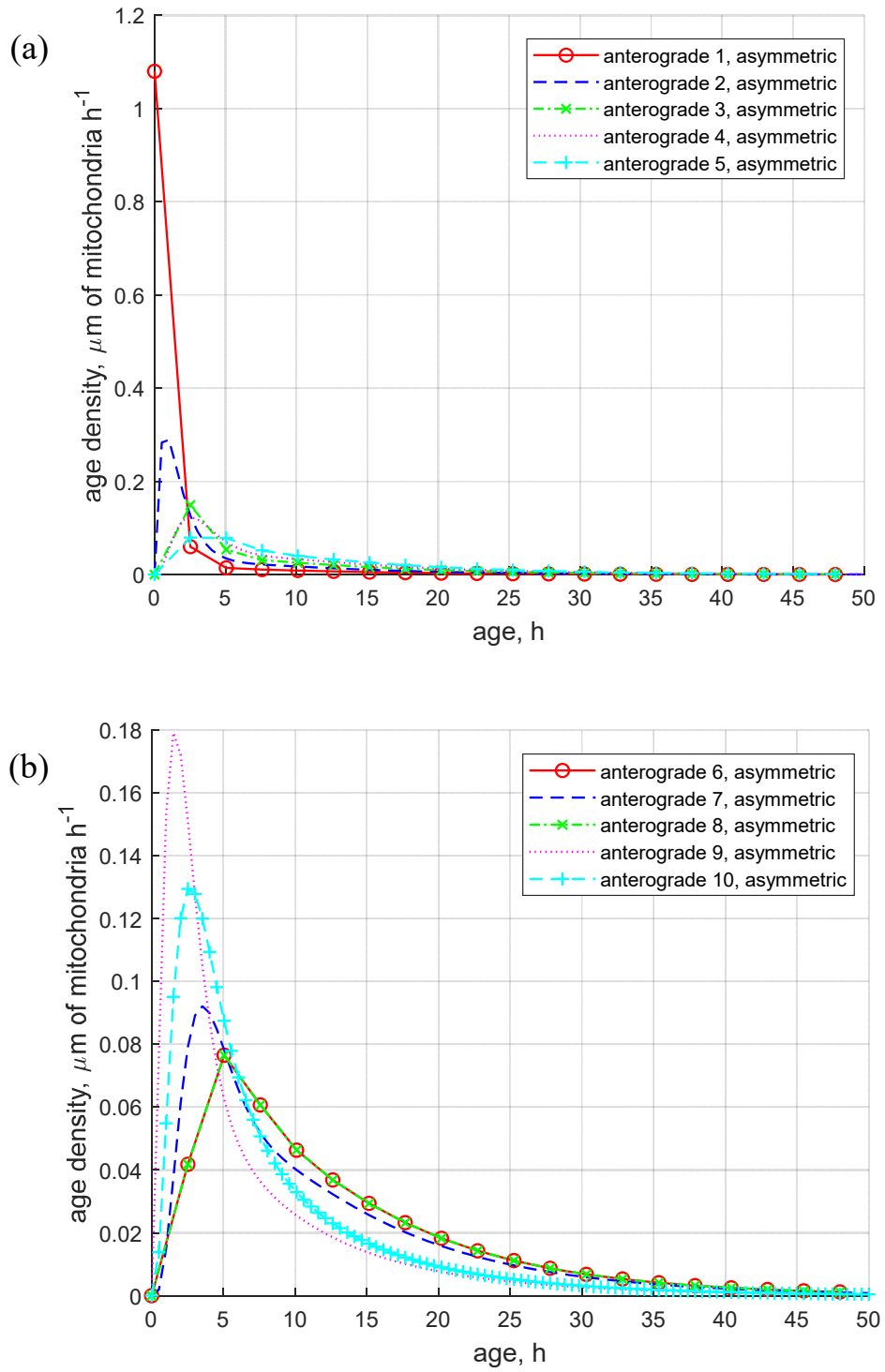

Fig. S4. Age density distributions of anterogradely moving mitochondria in an asymmetric branched axon across various demand sites. (a) Demand sites 1 to 7; (b) Demand sites 8 to 10.

(a)

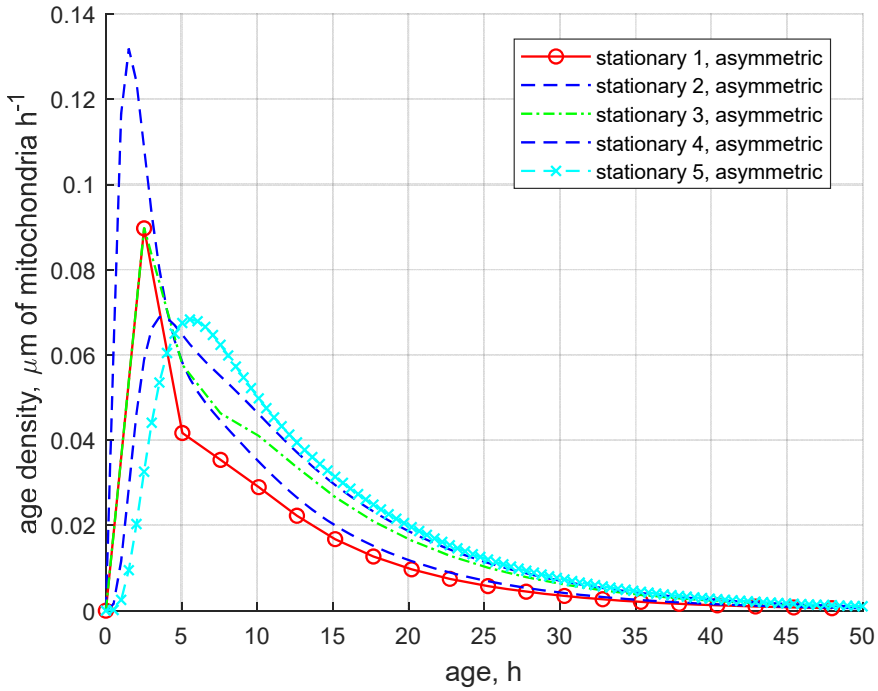
stationary 1, asymmetric
stationary 2, asymmetric
stationary 3, asymmetric
stationary 4, asymmetric
stationary 5, asymmetric
age density, μm of mitochondria h-1
age, h
0.14
0.12
0.1
0.08
0.06
0.04
0.02
0
0
5
10
15
20
25
30
35
40
45
50

(b)

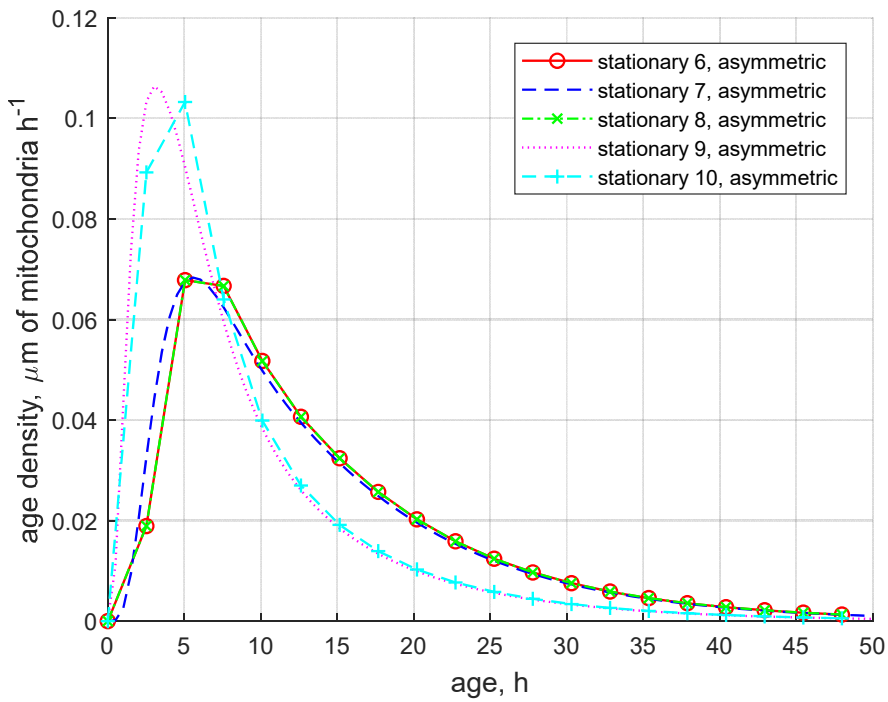
stationary 6, asymmetric
stationary 7, asymmetric
stationary 8, asymmetric
stationary 9, asymmetric
stationary 10, asymmetric
age density, μm of mitochondria h-1
age, h
0.12
0.1
0.08
0.06
0.04
0.02
0
0
5
10
15
20
25
30
35
40
45
50

Fig. S5. Age density distributions of stationary mitochondria in an asymmetric branched axon across various demand sites. (a) Demand sites 1 to 7; (b) Demand sites 8 to 10.

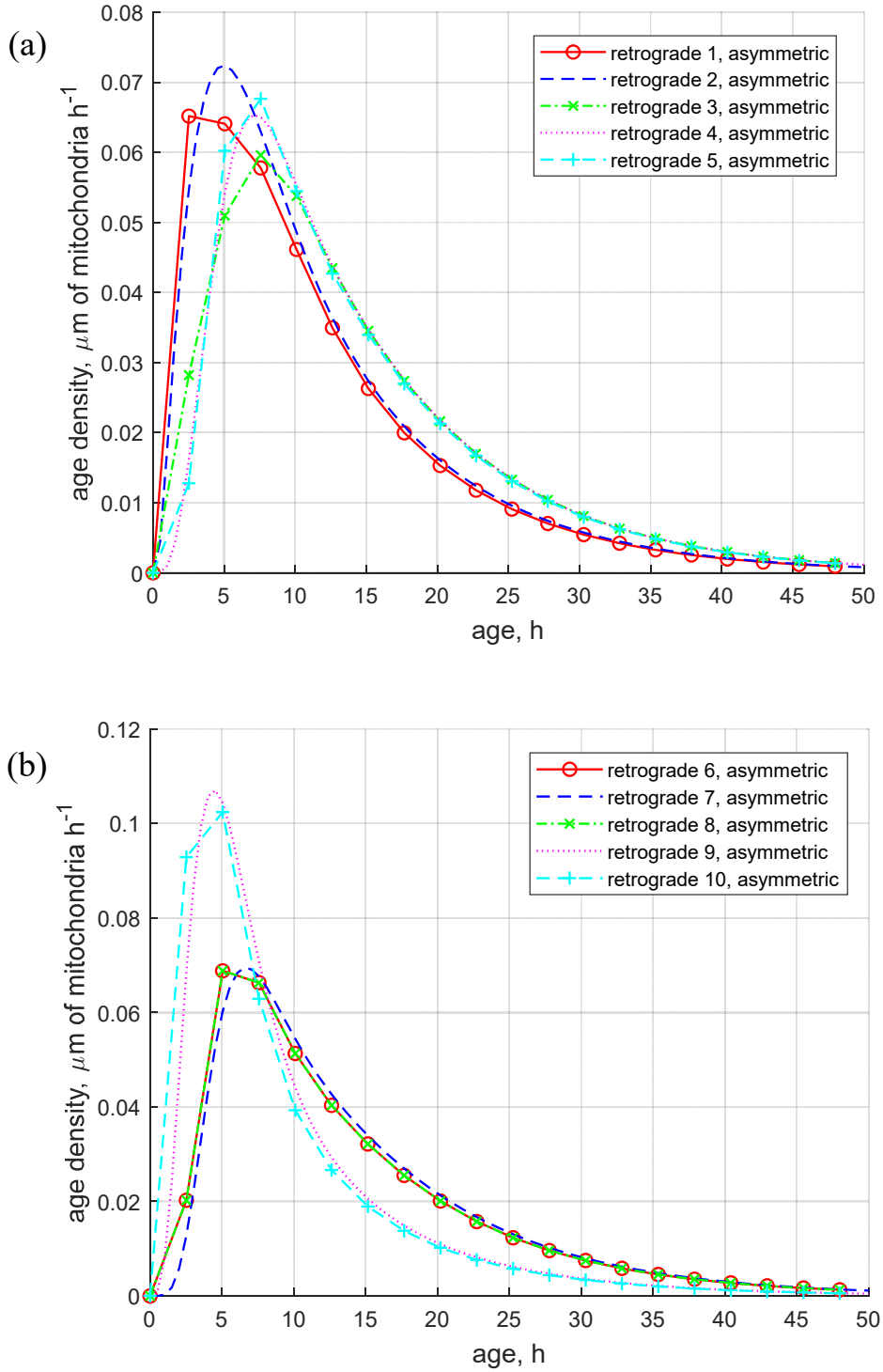

Fig. S6. Age density distributions of retrogradely moving mitochondria in an asymmetric branched axon across various demand sites. (a) Demand sites 1 to 7; (b) Demand sites 8 to 10.